come than in the non-HCV course.[3,4] The transplanted liver in HCV-related disease undergoes a rapid progression of fibrosis and worsens to cirrhosis and graft failure.[5] The factors for a worsening outcome were speculated to be increased donor age,[3-5] stronger immunosuppression,[3] and high levels of HCV-ribonucleic acid (RNA) at transplantation.[4] These factors have no small effect on the reinfection and reactivation of HCV in the graft liver.

Reinfection of HCV in the graft liver is rapid after transplantation, and the virus immediately proliferates in the graft. In the natural course of reinfection, approximately 10 to 25% of recipients will develop cirrhosis, and a strategy for the prevention of reinfection has not been developed.[6] At present, treatment of HCV after transplantation is inadequate, and does not result in a cure.[7] Recently, pegylated interferon (IFN) and ribavirin combination therapy has been effective in the treatment of HCV genotype 1a chronic hepatitis, with a sustained viral response rate of 45%.[8] However, reinfection after transplantation is the norm despite combined therapy.[9,10] Meanwhile, the patients with a sustained viral response after transplantation show no progression or reversal of liver fibrosis.[11,12] The refractory nature of pegylated IFN and ribavirin combination therapy for liver transplantation patients contributes to a worsening outcome in HCV-related transplantation.

We speculated that posttransplantation immunosuppression is part of the reason for IFN resistance to HCV reinfection of the graft liver. Methylprednisolone pulse therapy is a risk factor for severe outcome after transplantation, and the treatment of acute cellular rejection using heavy immunosuppressive agents is also a risk factor.[3,4,6] Previous reports described the fact that glucocorticoid inhibits the expression of signal transducers and activators of transcription (STAT)-1, as a signal transduction factor of IFN, and diminishes the signaling of IFN.[13] However, the effects on HCV reinfection and IFN therapy by calcineurin inhibitors, the most frequently used immunosuppressants, have not been fully evaluated, until now. Therefore, we have attempted to evaluate the influences of calcineurin inhibitors on IFN signaling in the hepatocytes.

IFN-α and β, after binding to their receptors, stimulate the intracellular IFN-signaling cascade including the Janus kinase (Jak)-STAT tyrosine kinases, the phosphorylation of STAT-1 and -2, and the formation of IFN-stimulated gene factor 3 (ISGF-3), which consists of STAT-1, STAT-2, and p48.[14] ISGF-3 translocates into the nucleus and binds to the IFN-stimulated regulatory element (ISRE) in the promoter sequences of a variety of IFN-inducible genes, including antiviral proteins such as double-stranded RNA-dependent protein kinase (PKR).[15] Several negative regulation systems of Jak-STAT signaling, including the suppressor of cytokines signaling family, the protein inhibitor of activated STAT family, and the SH2-containing protein tyrosine phosphatase family, are notorious contributors to a state of inflammation and carcinogenesis in the hepatocyte.[16,17] In addition, the nucleus-cytoplasm transport of ISGF-3 was regulated by translocated specific proteins along with the phosphorylation of STAT.[18] We examined the influence of calcineurin inhibitors on IFN-induced phosphorylation of Jak and STAT, nuclear translocation of ISGF-3, ISRE contained promoter activity, and the expressions of antiviral proteins.

MATERIALS AND METHODS

Reagents and Cell Culture

Recombinant human IFN-α2b, tacrolimus (Tac), and cyclosporine A (CyA) were generous gifts from Schering-Plough KK (Tokyo, Japan), Astellas Co. (Tokyo, Japan), and Novartis Pharma Co. (Basel, Switzerland), respectively. Hc human hepatocyte cells (Applied Cell Biology Research Institute, Kirkland, WA) and HuH-7 human hepatoma cells (American Type Culture Collection, Rockville, MD) were maintained in a chemically-defined medium, CS-C completed (Cell Systems, Kirkland, WA) and RPMI (Invitrogen, Grand Island, NY), respectively, supplemented with 5% fetal bovine serum. In the pretreatment of calcineurin inhibitors, the cells were cultured in 5% RPMI containing varying concentrations of Tac and CyA, and then the medium was exchanged and the cells were treated with IFN 100 IU/mL at the indicated time.

HCV Replicon System

OR6 cells stably harboring the full-length genotype 1 replicon, ORN/C-5B/KE[19] were used to examine the influence on the anti-HCV effect of IFN of calcineurin inhibitors. The cells were cultured in Dulbecco's modified Eagle's medium (Gibco-BRL; Invitrogen) supplemented with 10% fetal bovine serum, penicillin, and streptomycin and maintained in the presence of G418 (300 mg/L; Geneticin; Invitrogen). This replicon was derived from the 1B-2 strain (strain HCV-o, genotype 1b), in which the *Renilla* luciferase gene is introduced as a fusion protein with neomycin to facilitate the monitoring of HCV replication. After the treatment, the cells were harvested with *Renilla* lysis reagent (Promega, Madison, WI) and subjected to luciferase assay according to the manufacturer's protocol.

Western Blotting and Antibody

Western blotting with anti-PKR, anti-STAT-1, anti-STAT-2 (Santa Cruz Biotechnology, Santa Cruz, CA), anti-tyrosine-701 phosphorylated STAT-1, anti-tyrosine-689 STAT-2, anti-JAK-1 or anti-tyrosine 1022/1023 JAK-1 (New England Biolabs, Beverly, MA) was performed as described previously.[20] Briefly, Hc cells were lysed by the addition of lysis buffer (50 mmol/L Tris-HCl, pH 7.4, 1% Np40, 0.25% sodium deoxycholate, 0.02% sodium azide, 0.1% sodium dodecyl sulfate buffer, 150 mmol/L NaCl, 1 mmol/L ethylene diamine tetraacetic acid, 1 mmol/L phenylmethanesulfonylfluoride, 1 μg/mL each of aprotinin, leupeptin, and pepstatin, 1 mmol/L sodium o-vanadate, and 1 mmol/L NaF). Extraction of nucleus and cytoplasm were performed using the NE-PER Nuclear and Cyto-

plasmic Extraction kit (Pierce, France). Samples were analyzed by electrophoresis on 8 to 12% sodium dodecyl sulfate buffer polyacrylamide gel and electrotransferred to nitrocellulose membranes, and then blotted with each antibody. The membranes were incubated with horseradish peroxidase-conjugated anti-rabbit immunoglobulin G or anti-mouse immunoglobulin G, and the immunoreactive bands were visualized by the ECL chemiluminescence system (Amersham Life Science, Buckinghamshire, England). The density of each band was quantified using the National Institutes of Health image analysis software program.

Reporter Gene Assay

pISRE-Luc containing 5 copies of the ISRE sequence and firefly luciferase gene and pRL-SV40 containing SV40 early enhancer/promoter and *Renilla* luciferase gene were obtained from Clontech (San Diego, CA) and Promega, respectively. The HuH-7 cells were grown in 24-well multiplates and transfected with 1 μg of pISRE-Luc and 10 ng of pRL-SV40 as a standard by the lipofection method. One day later, the cells were incubated in the absence or presence of varying concentrations of Tac, CyA, and IFN-α, and the luciferase activities in the cells were determined using a dual-luciferase reporter assay system and a TD-20/20 luminometer (Promega). The data were expressed as the relative ISRE-luciferase activity.

Fluorescence Immunohistochemistry

The Hc cells were seeded onto 11-mm glass coverslips in 24-well plates at 240,000 cells/well. The next day, the medium was replaced with serum-free medium, and the cells were pretreated with 10 μmol/L of Tac, 100 μmol/L of CyA, or vehicle, for 16 hours and then stimulated with 100 IU/mL of IFN-α for 10 minutes. Fluorescence immunohistochemistry was performed as described previously.[21] The cells were incubated with anti-tyrosine-701 phosphorylated STAT-1 antibody for 1 hour at room temperature, washed 3 times in phosphate buffered saline, incubated with rhodamine-conjugated donkey anti-rabbit immunoglobulin G (Jackson ImmunoResearch Laboratories, Inc., West Grove, PA) for 1 hour, washed in phosphate buffered saline, and mounted in Vectashield Mounting Medium (Vector Laboratories Inc., Burlingame, CA). Nuclear staining was performed using Hoechst 33258 (Invitrogen Japan K.K., Tokyo, Japan). Immunofluorescence analysis was done by an Olympus BX50 microscope (Tokyo, Japan) and the image was captured by a Nikon DXM 1200 digital camera (Tokyo, Japan).

RESULTS

Differential Effects of Tac and CyA on IFN-induced Antiviral Protein Expression

To elucidate how calcineurin inhibitors exert influence on IFN-induced antiviral protein, the Hc cells were incubated in the absence or presence of IFN-α after the presence or absence of pretreatment of Tac (Fig. 1A) or CyA (Fig. 1B) for 16 hours, and then were harvested for the western blot analysis. Pretreated Tac had an inhibitory effect on IFN-α-induced PKR expression, antiviral protein as messenger RNA translation inhibitor activated by double-stranded RNA dependent, in a dose-dependent manner, but no inhibitory effect of pretreatment CyA for PKR expression was recognized in our experiment. STAT-1 is an essential signal transmitter substance of IFN and IFN-inducible proteins.

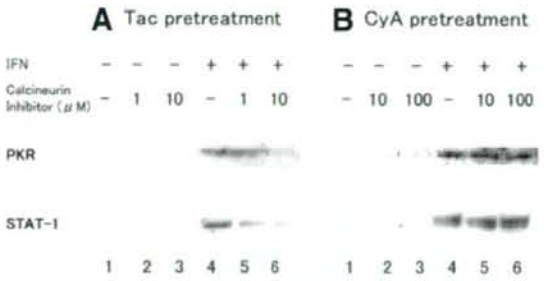

Figure 1. Effect of (A) Tac and (B) CyA on IFN-α-induced PKR and STAT-1. Hc cells were treated with 100 IU/mL of IFN-α in the absence (lane 4) or presence of pretreatment (lanes 5 and 6). Indicated concentration of calcineurin inhibitor alone was lanes 2 and 3, lane 1 was not treated with IFN-α and calcineurin inhibitors. One day later, PKR and STAT-1 were determined by western blotting.

The expression of IFN-inducible STAT-1 also decreased in a dose-dependent manner after the administration of Tac, but not after the administration of CyA.

Alterations of IFN-α-Stimulated Reporter Gene Expression by Tac and CyA

Because the formation of IFN stimulating gene factor (ISGF) 3 by IFN-α leads to transactivation of the ISRE in the promoter regions of the IFN-α-inducible genes, we performed the reporter gene transfection assay using plasmids containing ISRE in their promoter sequence. Because there were not enough Hc cells for reporter gene transfection, we used HuH-7 cells in the transfection assay. HuH-7 cells were transfected with pISRE-Luc containing 5 repeats of ISRE sequence and pRV-SV40 as a standard and then were treated with IFN-α after 16 hours in the presence or absence of pretreated Tac or CyA (Fig. 2). Tac and CyA alone did not influence the ISRE-luciferase activities. IFN-α combined with Tac and attenuated its expression compared with IFN-α alone. In contrast, there was a slight attenuation effect of its expression in 100 μmol/L of pretreated CyA.

Inhibitory Effect of Tac on IFN-α-Induced Tyrosine Phosphorylation of STATs

The activation of STAT-1 and -2 by phosphorylation of tyrosine-701 and 689 residues, respectively, is essential for the relay of IFN-α signal with the formation of ISGF-3. Therefore, we examined the effect of Tac and CyA on the IFN-α-induced tyrosine phosphorylation of

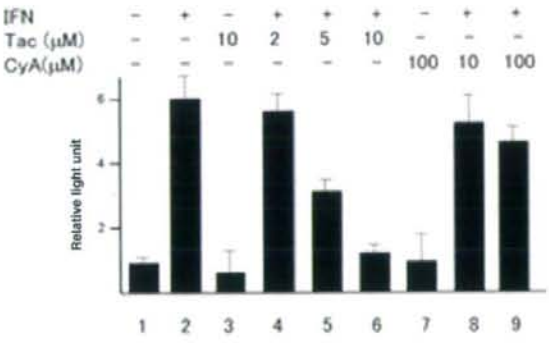

Figure 2. Suppression effect of calcineurin inhibitors on IFN-α-induced reporter gene assay. HuH-7 cells transfected with reporter gene (pISRE-Luc and pRL-SV40) were either untreated (lanes 1, 2) or pretreated with Tac (lanes 3-6) or CyA (lanes 7-9) for 16 hours, followed by IFN-α 100 IU/mL (lanes 2, 4-6, 8, and 9)or absence (lanes 3 and 7). Six hours later, the relative ISRE-luciferase activity (n = 4) was determined as described in Materials and Methods. The data are expressed as the mean ± SD and are representative examples of four similar experiments.

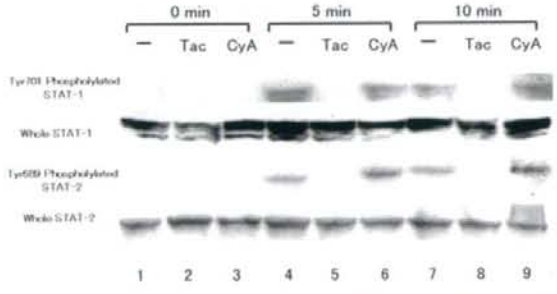

Figure 3. Effect of calcineurin inhibitors on STAT-1and STAT-2. After pretreatment with 10 μmol/L Tac (lanes 2, 5, and 8) and 100 μmol/L CyA (lanes 3, 6, and 9) for 16 hours, Hc cells were untreated (lane 1) or treated with 100 IU/mL IFN-α (lanes 4-9) for the indicated periods and phosphorylated STAT-1 at tyrosine-701 residue (first panel), expression of STAT-1 (second panel), phosphorylated STAT-2 at tyrosine-689 residue (third panel), and expression of STAT-2 (fourth panel) were analyzed by western blotting. The density of each band was quantified and the nuclear translocation rate was calculated by the following: nuclear intensity (N)/[nuclear intensity (N) + cytoplasmic intensity (C)].

STAT-1 and -2 (Fig. 3). IFN-α clearly induced the tyrosine phosphorylation of STAT-1 and -2, but Tac and CyA could not. However, when the Hc cells were pretreated with Tac, but not CyA, before IFN-α stimulation, the levels of tyrosine phosphorylated STAT-1 and -2 were clearly lower than those induced by IFN-α alone. In the case of pretreatment with CyA, the IFN-α-induced tyrosine phosphorylation levels were similar to IFN-α alone. Then, the cells were changed from Hc cells to HuH-7 cells and a similar experiment was done. The inhibitory effect of Tac to IFN-α-induced STAT-1 and -2 tyrosine phosphorylation was the same (data not shown).

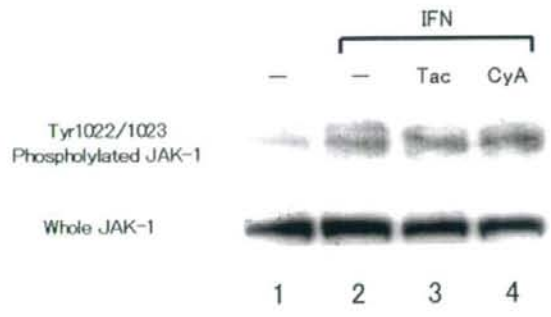

Figure 4. Evaluation of IFN-α-induced phosphorylated JAK-1 by calcineurin inhibitors. After pretreatment of 10 μmol/L Tac (lane 3) and 100 μmol/L CyA (lane 4) for 16 hours, Hc cells were untreated (lane 1) or treated with 100 IU/mL IFN-α (lanes 2-4) for 3 minutes, then phosphorylated JAK-1 at tyrosine-1022/1023 residue (first panel) and expression of JAK-1 (second panel) were analyzed by western blotting.

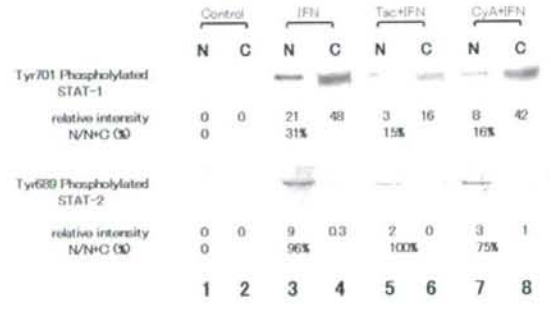

Figure 5. Alternation of distribution of IFN-α-induced phosphorylated STAT-1 and STAT-2 by calcineurin inhibitors. Hc cells were pretreated with absence (lanes 1-4) or presence of 10 μmol/L Tac (lanes 5 and 6) or 100 μmol/L CyA (lanes 7 and 8). And then, Hc cells were stimulated by 500 IU/L IFN-α (lanes 3-8) for 10 minutes. Hc cells harvested by extraction kit of nucleus (lanes 1, 3, 5, and 7) and cytoplasm (lanes 2, 4, 6, and 8). Phosphorylated STAT-1 at tyrosine-701 residue (upper panel) and phosphorylated STAT-2 at tyrosine-689 residue (lower panel) were analyzed by western blotting.

When we performed western blotting of phosphorylated JAK-1 under the same conditions, Tac and CyA did not decrease the IFN-induced JAK-1 phosphorylation (Fig. 4).

Influence of Calcineurin Inhibitors on IFN-α-Induced Nuclear Translocation of Tyrosine Phosphorylated STATs

For transcription of the IFN-α-induced antiviral gene, the ISGF-3 complex, including activated STAT-1, STAT-2, and p48, could be translocated to the nucleus. Initially, we detected tyrosine phosphorylated STAT-1 and -2 extracted it from the nucleus and cytoplasm by western blotting. In this experiment, detectable band intensities were quantified by National Institutes of Health image software and we evaluated the nuclear translocation rate of activated STAT-1 and -2 (Fig. 5).

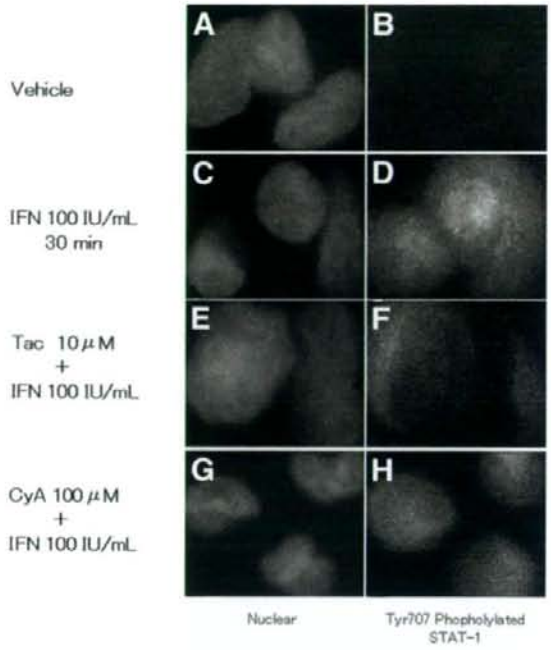

Figure 6. Inhibition of IFN-α-induced nuclear translocation of phosphorylated STAT-1 by calcineurin inhibitor. Hc cells were pretreated in the absence (A-D) or presence of 10 μmol/L Tac (E,F) or 100 μmol/L CyA (G,H). After pretreatment, Hc cells were stimulated by 100 IU/L IFN-α (C-H) for 30 minutes. Thereafter, the cells were fixed, permeabilized, processed for immunofluorescence (B,D,F,H) and Hoechst staining (A,C,E,G), and visualized with fluorescence microscopy. The results shown are from one representative experiment from a total of three performed.

The total IFN-α-stimulated tyrosine phosphorylated STAT-1 was decreased by pretreatment with Tac; furthermore, the nuclear translocation rate of activated STAT-1 was inhibited both by pretreatment with Tac and CyA. However, in the case of pretreatment with Tac and CyA, there was no effect on the nuclear translocation of tyrosine phosphorylated STAT-2. Secondarily, we evaluated the location of tyrosine phosphorylated STAT-1 by fluorescence immunohistochemistry of cultured Hc cells (Fig. 6).The IFN-α-induced nuclear translocation of tyrosine phosphorylated STAT-1 was observed, but its translocation was inhibited by pretreatment with Tac. Along with the nuclear translocation rate of activated STAT-1 by western blotting (Fig. 5), pretreatment with Tac also attenuated the nuclear staining of activated STAT-1 compared to IFN-α alone, but did not attenuate the expression of activated STAT-1 by immunohistochemistry.

Inhibitory Effect of Tac on IFN-α-Induced Anti-HCV Efficiency

To examine the effect of calcineurin inhibitors on IFN-α, we used the full-length HCV replication system, OR6 cells. The cells were treated with IFN-α after 16 hours in

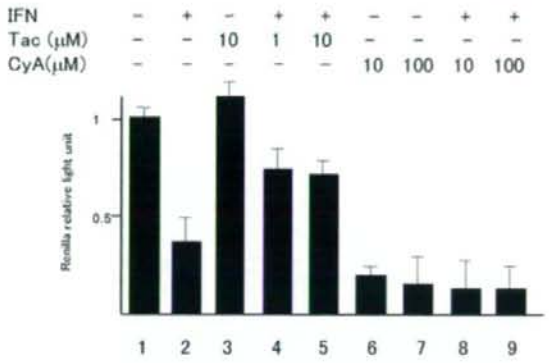

Figure 7. Alternation of IFN-α-suppressed HCV replication by Tac. OR6 cells, full-length replicon system, were treated with 100 IU/mL of IFN-α in the absence (lane 2) or presence of pretreatment (lanes 4, 5, 8, and 9). Indicated concentration of calcineurin inhibitor alone was lanes 3, 6, and 7, lane 1 was not treated with IFN-α and calcineurin inhibitors. One day later, *Rennila* luciferase activity was determined by luminometer.

the presence or absence of pretreated Tac or CyA (Fig. 7). IFN-α or CyA alone repressed the *Renilla* luciferase activity, which is well correlated with HCV-RNA concentration in OR6 cells.[19] In contrast, Tac alone had little effect on *Renilla* luciferase activity. However, pretreatment with Tac attenuated the IFN-α-induced repression of *Renilla* luciferase activity (Fig. 7; lane 2 versus lanes 4 and 5), but pretreatment with CyA did not (Fig. 7; lanes 8 and 9).

DISCUSSION

We herein show that calcineurin inhibitors, especially Tac, are negative regulators of IFN signaling in the hepatocyte, and the greatest cause of this phenomenon is phosphorylation of STAT-1, next to inhibition of nuclear translocation of STAT-1. Disturbance of STAT-1 phosphorylation caused diminished ISRE-containing promoter activity, for example PKR and STAT-1, and antiviral protein expression declined. Pretreatment with Tac diminished the replication inhibitory effect of IFN-α. This phenomenon has a detrimental effect on IFN therapy after HCV-related liver transplantation. In our experiments, we speculated that Tac is not better suited for posttransplantation IFN therapy than CyA, but it did not report that IFN-a response is different between Tac and CyA in human study in previous time. When the alternative of potent immunosuppressant for prevention of rejection, or antiviral-activity for HCV reactivation is weighed, we might need to consider other factors in choosing between Tac and CyA. We had compared high concentration CyA with low concentration Tac, since rejection was controlled by serum trough values of tacrolimus of 5 ng/mL and of cyclosporin of 100 ng/mL in our hospital in the period of stability after liver transplantation.

Recently, the difference between Tac and CyA has been regarded in another function than immunosuppression, and we presume that this discrepancy de-

pended on differences of "immunophilins." Immunophilins are a ubiquitous family of proteins. All cells contain several members of this family, which bind specific calcineurin inhibitors and participate in many cellular functions.[22] Tac has been reported to have neuroprotection,[23] but CyA did not, whereas CyA had anti-HCV action,[24-26] but Tac did not. Tac binds specific FK506 binding protein members of the immunophilin family, whereas cyclosporin binds a different subset of immunophilins (cyclophilins). FK506 binding protein and CyP have the same function as peptidyl prolyl *cis-trans* isomerase and they inhibited the nuclear translocation of nuclear factor of activated T cells (NF-AT). Despite this common pathway, the cell protection activity has been reported to require the induction of heat shock protein 70 by Tac but not CyA,[27] and the anti-HCV activity contributed to a specific blockade of CyP B by CyA.[25] The differences in the medical effects for immunosuppression between Tac and CyA require attention, when these immunosuppressants are used in posttransplantation-related HCV infection.

In our study, the IFN-induced tyrosine phosphorylated STAT-1 and -2 both decreased after the administration of Tac, but Tac is known essentially for the inhibition of serine/threonine protein phosphatase. Calcineurin, regardless of independent Jak-1 tyrosine phosphorylation, and CyA did not have such a tyrosine phosphatase action against STAT-1 and -2. We could not resolve this phosphatase mechanism, but we speculated that Tac induced the tyrosine phosphatase kinase and inhibited tyrosine phosphorylation of STAT-1 and -2. Tac did not induce suppression of cytokines signaling-1 and 3, Jak inhibitors, by western blotting in our study (data not shown); however, we could not rule out the induction of other types of tyrosine phosphatase. Previous studies described that suppressor of cytokines signaling-1, 3 and SH2-containing protein tyrosine phosphatase inhibited NF-AT activation,[28-30] and therefore the relationship between Tac and tyrosine phosphatase might be reconsidered. Barat and Tremblay[31] and Zhu and McKeon[32] previously described the protein-tyrosine phosphatase inhibitor bisperoxovanadium as a potent activator of T cell receptor signaling, and SH2-containing protein tyrosine phosphatase-1, T cell protein-tyrosine phosphatase, Tac, and CyA are inhibitors of such activation. We were interested in the inhibition of protein-tyrosine phosphatase inhibitor by Tac and CyA, because Tac and CyA possessed the same action as SH2-containing protein tyrosine phosphatase-1 and protein-tyrosine phosphatase.[32] Furthermore, this action of Tac was stronger than CyA.[31] From these studies, we assume that Tac has tyrosine phosphatase action in the hepatocyte and inhibits tyrosine phosphorylation of STAT-1 and -2.

The inhibition of IFN-induced antiviral proteins by Tac, and the inhibition of nuclear trafficking of tyrosine phosphorylated STAT-1, is the common phenomenon between Tac and CyA in this study. This phenomenon was observed in the western blotting findings (Fig. 3) and immunohistochemistry of the cultured cells (Fig. 6).

NF-AT activation requires the suppression of Crm1-dependent export from nucleus to cytoplasm by calcineurin,[33] and the presence of importin, bounded to calcineurin, in the nucleus.[34] In IFN-induced Jak-STAT signaling, nuclear trafficking of ISGF-3 requires suppression of Crm1 and binding importin[18] in the same fashion as NF-AT. Calcineurin inhibitors bind to immunophilin and inhibit dephosphorylation of NF-AT, then they inhibit the transcription activity of NF-AT. In addition to such action, it might be considered that the nuclear trafficking of NF-AT is regulated by the calcineurin inhibitor and immunophilin complex. We speculated that the decrease of the nuclear import of tyrosine phosphorylated STAT-1 is the function, the calcineurin inhibitor and immunophilin complex modified Crm1 and importin in the same fashion as NF-AT. Then, we recognized that the mechanisms of diminished tyrosine phosphorylation STATs and nuclear translocation STAT-1 were different.

Presently, there is no definite opinion regarding the selection of calcineurin inhibitors for liver transplantation.[6] However, reports of inhibition of HCV replication by CyA in vitro were noted recently[24-26] and the result were same in our full-length replicon system (Fig. 7). In our data, we consider that CyA has the effect of, not only the previously reported anti-HCV replication action itself, but it creates much less interference with IFN treatment for HCV reactivated after liver transplantation than does Tac. It has been reported that CyA increased the chance of a sustained viral response after liver transplantation.[35] However, we used care with our data, because both Tac and CyA inhibit the nuclear translocation of tyrosine phosphorylated STAT-1. Our data revealed that when an excess of CyA was used after liver transplantation, it resulted in a decrease in the amount of IFN-induced antiviral protein, because of inhibition of nuclear transportation of tyrosine phosphorylation STAT-1 (Figs. 5 and 6). The immunosuppression levels of Tac and CyA have already been reported to decrease significantly in patients responding favorably to anti-HCV therapy post–liver transplantation.[36] In this study, we therefore considered it necessary to pay attention to an excess dose of CyA, when IFN treatment for reactivation of HCV is required.

In conclusion, Tac has been shown to influence the tyrosine phosphorylation of STAT-1, and the result was a decline in antiviral protein PKR. In addition, Tac and CyA have been shown to interfere with the translocation of STAT-1. We speculated that posttransplantation immunosuppression is part of the reason for IFN resistance to HCV reinfection of the graft liver. As the course, calcineurin inhibitors, especially Tac, were pointed out in this study, and we clarified a part of the IFN resistance. Although the mechanism of inhibition of IFN signaling has not yet been fully investigated, it is necessary to compare the antirejection action of Tac to the anti-HCV action of CyA when selecting calcineurin inhibitors.

REFERENCES

1. Perz JF, Armstrong GL, Farrington LA, Hutin YJ, Bell BP. The contributions of hepatitis B virus and hepatitis C virus

infection to cirrhosis and primary liver cancer worldwide. J Hepatol 2006;45:529-538.
2. Forman LM, Lewis JD, Berlin JA, Feldman HI, Lucey MR. The association between hepatitis C infection and survival after orthotopic liver transplantation. Gastroenterology 2002;122:889-896.
3. Berenguer M, Prieto M, San Juan F, Rayon JM, Martinez F, Carrasco D, et al. Contribution of donor age to the recent decrease in patient survival among HCV-infected liver transplant recipients. Hepatology 2002;36:202-210.
4. Berenguer M, Ferrell L, Watson J, Prieto M, Kim M, Rayon M, et al. HCV-related fibrosis progression following liver transplantation: increase in recent years. J Hepatol 2000; 32:673-684.
5. Berenguer M, Crippin J, Gish R, Bass N, Bostrom A, Netto G, et al. A model to predict severe HCV-related disease following liver transplantation. Hepatology 2003;38:34-41.
6. Everson GT. Impact of immunosuppressive therapy on recurrence of hepatitis C. Liver Transpl 2002;8:S19–S27.
7. Gane E. Treatment of recurrent hepatitis C. Liver Transpl 2002;8:S28–S37.
8. Davis GL, Wong JB, McHutchison JG, Manns MP, Harvey J, Albrecht J. Early virologic response to treatment with peginterferon alfa-2b plus ribavirin in patients with chronic hepatitis C. Hepatology 2003;38:645-652.
9. Castells L, Vargas V, Allende H, Bilbao I, Luis Lazaro J, Margarit C, et al. Combined treatment with pegylated interferon (alpha-2b) and ribavirin in the acute phase of hepatitis C virus recurrence after liver transplantation. J Hepatol 2005;43:53-59.
10. Heydtmann M, Freshwater D, Dudley T, Lai V, Palmer S, Hubscher S, et al. Pegylated interferon alpha-2b for patients with HCV recurrence and graft fibrosis following liver transplantation. Am J Transplant 2006;6:825-833.
11. Bizollon T, Pradat P, Mabrut JY, Chevallier M, Adham M, Radenne S, et al. Benefit of sustained virological response to combination therapy on graft survival of liver transplanted patients with recurrent chronic hepatitis C. Am J Transplant 2005;5:1909-1913.
12. Abdelmalek MF, Firpi RJ, Soldevila-Pico C, Reed AI, Hemming AW, Liu C, et al. Sustained viral response to interferon and ribavirin in liver transplant recipients with recurrent hepatitis C. Liver Transpl 2004;10:199-207.
13. Hu X, Li WP, Meng C, Ivashkiv LB. Inhibition of IFN-gamma signaling by glucocorticoids. J Immunol 2003; 170:4833-4839.
14. Kimura T, Kadokawa Y, Harada H, Matsumoto M, Sato M, Kashiwazaki Y, et al. Essential and non-redundant roles of p48 (ISGF3 gamma) and IRF-1 in both type I and type II interferon responses, as revealed by gene targeting studies. Genes Cells 1996;1:115-124.
15. Kuhen KL, Vessey JW, Samuel CE. Mechanism of interferon action: identification of essential positions within the novel 15-base-pair KCS element required for transcriptional activation of the RNA-dependent protein kinase pkr gene. J Virol 1998;72:9934-9939.
16. Brierley MM, Fish EN. Stats: multifaceted regulators of transcription. J Interferon Cytokine Res 2005;25:733-744.
17. Ogata H, Kobayashi T, Chinen T, Takaki H, Sanada T, Minoda Y, et al. Deletion of the SOCS3 gene in liver parenchymal cells promotes hepatitis-induced hepatocarcinogenesis. Gastroenterology 2006;131:179-193.
18. Reich NC, Liu L. Tracking STAT nuclear traffic. Nat Rev Immunol 2006;6:602-612.
19. Ikeda M, Abe K, Dansako H, Nakamura T, Naka K, Kato N,. Efficient replication of a full-length hepatitis C virus genome, strain O, in cell culture, and development of a luciferase reporter system. Biochem Biophys Res Commun 2005;329:1350-1359.
19. Ichikawa T, Nakao K, Nakata K, Yamashita M, Hamasaki K, Shigeno M, et al. Involvement of IL-1beta and IL-10 in IFN-alpha-mediated antiviral gene induction in human hepatoma cells. Biochem Biophys Res Commun 2002; 294:414-422.
20. Nishimura D, Ishikawa H, Matsumoto K, Shibata H, Motoyoshi Y, Fukuta M, et al. DHMEQ, a novel NF-kappaB inhibitor, induces apoptosis and cell-cycle arrest in human hepatoma cells. Int J Oncol 2006;29:713-719.
21. Takahashi N. Macrolide compounds as inhibitors of the intracellular signal transmission pathway: the mechanism of actions of rapamycin and FK506. Jpn J Antibiot 2000;53(Suppl A):62-67.
22. Keswani SC, Chander B, Hasan C, Griffin JW, McArthur JC, Hoke A. FK506 is neuroprotective in a model of antiretroviral toxic neuropathy. Ann Neurol 2003;53:57-64.
23. Watashi K, Hijikata M, Hosaka M, Yamaji M, Shimotohno K. Cyclosporin A suppresses replication of hepatitis C virus genome in cultured hepatocytes. Hepatology 2003; 38:1282-1288.
24. Watashi K, Ishii N, Hijikata M, Inoue D, Murata T, Miyanari Y, Shimotohno K. Cyclophilin B is a functional regulator of hepatitis C virus RNA polymerase. Mol Cell 2005; 19:111-122.
25. Henry SD, Metselaar HJ, Lonsdale RC, Kok A, Haagmans BL, Tilanus HW, et al. Mycophenolic acid inhibits hepatitis C virus replication and acts in synergy with cyclosporin A and interferon-alpha. Gastroenterology 2006;131:1452-1462.
26. Kaibori M, Inoue T, Tu W, Oda M, Kwon AH, Kamiyama Y, et al. FK506, but not cyclosporin A, prevents mitochondrial dysfunction during hypoxia in rat hepatocytes. Life Sci 2001;69:17-26.
27. Matsuda T, Yamamoto T, Kishi H, Yoshimura A, Muraguchi A. SOCS-1 can suppress CD3zeta- and Syk-mediated NF-AT activation in a non-lymphoid cell line. FEBS Lett 2000;472:235-240.
28. Banerjee A, Banks AS, Nawijn MC, Chen XP, Rothman PB. Cutting edge: suppressor of cytokine signaling 3 inhibits activation of NFATp. J Immunol 2002;168:4277-4281.
29. Su MW, Yu CL, Burakoff SJ, Jin YJ. Targeting Src homology 2 domain-containing tyrosine phosphatase (SHP-1) into lipid rafts inhibits CD3-induced T cell activation. J Immunol 2001;166:3975-3982.
30. Fortin JF, Barbeau B, Robichaud GA, Pare ME, Lemieux AM, Tremblay MJ. Regulation of nuclear factor of activated T cells by phosphotyrosyl-specific phosphatase activity: a positive effect on HIV-1 long terminal repeat-driven transcription and a possible implication of SHP-1. Blood 2001;97:2390-2400.
31. Barat C, Tremblay MJ. Treatment of human T cells with bisperoxovanadium phosphotyrosyl phosphatase inhibitors leads to activation of cyclooxygenase-2 gene. J Biol Chem 2003;278:6992-7000.
32. Zhu J, McKeon F. NF-AT activation requires suppression of Crm1-dependent export by calcineurin. Nature 1999; 398:256-260.
33. Hallhuber M, Burkard N, Wu R, Buch MH, Engelhardt S, Hein L, et al. Inhibition of nuclear import of calcineurin prevents myocardial hypertrophy. Circ Res 2006;99:626-635.
35. Firpi RJ, Zhu H, Morelli G, Abdelmalek MF, Soldevila-Pico C, Machicao VI, et al. Cyclosporine suppresses hepatitis C virus in vitro and increases the chance of a sustained virological response after liver transplantation. Liver Transpl 2006;12:51-57.
36. Kugelmas M, Osgood MJ, Trotter JF, Bak T, Wachs M, Forman L, et al. Hepatitis C virus therapy, hepatocyte drug metabolism, and risk for acute cellular rejection. Liver Transpl 2003;9:1159-1165.

Journal of Medical Virology 80:632–639 (2008)

Possible Molecular Mechanism of the Relationship Between NS5B Polymorphisms and Early Clearance of Hepatitis C Virus During Interferon Plus Ribavirin Treatment

Mitsuyasu Nakamura,[1] Hidetsugu Saito,[1]* Masanori Ikeda,[2] Shinichiro Tada,[1] Naoki Kumagai,[3] Nobuyuki Kato,[2] Kunitada Shimotohno,[4] and Toshifumi Hibi[1]

[1]*Division of Gastroenterology and Hepatology, Department of Internal Medicine, School of Medicine, Keio University, Shinanomachi, Shinjuku-ku, Tokyo, Japan*
[2]*Department of Molecular Biology, Okayama University Graduate School of Medicine and Dentistry, Shikada-cho, Okayama, Japan*
[3]*Research Center for Liver Diseases, The Kitasato Institute, Shirogane, Minato-ku, Tokyo, Japan*
[4]*Center for Integrated Medical Research, School of Medicine, Keio University, Shianomachi, Shinjuku-ku, Tokyo, Japan*

We previously reported the relationship between viral polymerase polymorphisms and the initial decline in viral load induced by interferon-α and ribavirin therapy in genotype 1b-related chronic hepatitis C patients. The presence of E124K and I85V of NS5B was closely associated with viral clearance at 8 weeks of treatment. The aim of this study was to investigate the mechanisms by which this polymorphism of NS5B protein affects early viral clearance. We used a replicon system derived from strain O, genotype 1b virus. Three mutants (V85I), (K124E), and (V85I/K124E) were introduced to the replicon. OR6c, a derivative of HuH7 cells, was transfected with the replicon including a luciferase reporter gene. Luciferase activities were measured 72 hr post-transfection. All three mutants showed higher luciferase activity than that of the wild type, and the V85I mutant showed the highest activity. This result was also confirmed by neomycin gene-containing replicons with same mutations. All replicons were down-regulated by ribavirin, but the level of reduction in the V85I mutant was the lowest. Our results suggested that this mutation at least partly contributes to resistance to early viral clearance during interferon and ribavirin combination therapy. ***J. Med. Virol. 80:632–639, 2008.***

KEY WORDS: hepatitis C virus; NS5B polymorphism; replicon; interferon and ribavirin combination therapy; viral proliferation

INTRODUCTION

With an estimated 170 million infected individuals, hepatitis C virus (HCV) has a major impact on public health. An estimated 65–80% of the individuals infected with HCV develop persistent infection while 20–50% develop cirrhosis and 5% develop hepatocellular carcinoma (HCC) [Liang et al., 2000; Gao et al., 2004]. Until recently, interferon (IFN)-α and IFN-β were the only available treatments for HCV infection, although only 10–15% of treated subjects achieved sustained viral eradication with IFN monotherapy, and early viral clearance after initiation of IFN monotherapy was correlated with sustained viral clearance [Saito et al., 2000].

The current approved treatment for HCV infection is pegylated IFN-α (peg-IFN) in combination with ribavirin (RBV). This combination therapy leads to viral clearance in 50–80% of cases, depending on the infecting HCV genotype, and 50% of patients with HCV genotype 1b and high baseline levels of viral RNA do not achieve a sustained virological response with the combination therapy after 48 weeks [Manns et al., 2001; Fried et al., 2002; Feld and Hoofnagle, 2005]. Several prior studies have attempted to predict the efficacy of IFN plus RBV combination therapy. A quantitative measurement of HCV viremia or the initial decline in viral load is a reliable marker for early prediction of the therapeutic response to IFN and RBV combination therapy [Zeuzem et al., 1998; Bouvier-Alias et al., 2002; Takahashi et al., 2005; Lukasiewicz et al., 2007].

RBV is a broad-spectrum nucleoside analogue antiviral drug which is especially noted for its actions

Grant sponsor: Viral Hepatitis Research Foundation of Japan.

*Correspondence to: Hidetsugu Saito, Department of Internal Medicine, School of Medicine, Keio University, 35 Shinanomachi, Shinjuku-ku, Tokyo 160-8582, Japan.
E-mail: hsaito@sc.itc.keio.ac.jp

Accepted 28 December 2007
DOI 10.1002/jmv.21125
Published online in Wiley InterScience (www.interscience.wiley.com)

against RNA viruses and exhibits in vitro activity against some DNA and RNA viruses, including certain members of *Flaviviridae* [Sidwell et al., 1972]. It has recently been demonstrated that the antiviral activity of RBV can result from the ability of a viral RNA-dependent RNA polymerase (RdRP) to utilize RBV triphosphate and to incorporate this nucleotide into the viral genome with reduced specificity, thereby mutagenizing the genome and decreasing the yield of infectious virus [Crotty et al., 2000; Lanford et al., 2003]. Moreover, RBV exhibits an antiviral effect through a mechanism of error-prone replication in the HCV subgenomic replication system [Contreras et al., 2002]. Although RBV by itself cannot decrease serum HCV RNA levels in patients, it has been demonstrated that combination therapy with RBV and either IFN-α or peg-IFN yields a higher sustained response rate than is achieved with IFN-α monotherapy [Pol et al., 2000; Poynard et al., 2000; Saracco et al., 2001].

We previously reported the relationship between viral RdRP polymorphisms and the initial decline in viral load induced by IFN-α and RBV therapy in genotype 1b-related chronic hepatitis C patients [Kumagai et al., 2004]. Substitution of glutamic acid to lysine at the 124th position (E124K) and of isoleucine to valine at the 85th position (I85V) of NS5B was closely associated with viral clearance at 8 weeks of treatment.

In this study, we used the genotype 1b HCV replicon system [Ikeda et al., 2005] to generate NS5B mutants (E124K, I85V, and both) and we compared the replication activity with that of the wild-type replicon and to analyze how this polymorphism of NS5B protein affects early viral clearance during combination therapy with IFN and RBV. We also examined the significance of NS5B polymorphisms in the RBV-induced decrease in viral replication. We concluded that the identified polymorphism of NS5B partly affects viral replication.

MATERIALS AND METHODS

Cell Culture System

OR6 cells were cultured in Dulbecco's modified Eagle's medium (Gibco-BRL, Invitrogen Life Technology, Carlsbad, CA) supplemented with 10% fetal calf serum, penicillin, and streptomycin (complete DMEM), in addition to G418 (300 μg/ml; Geneticin, Invitrogen), and were then passaged twice a week at a 5:1 split ratio. OR6c cells are cured OR6 cells from which genome-length HCV RNA was eliminated by IFN-α treatment (500 IU/ml for 2 weeks) without G418, as previously described [Ikeda et al., 2005].

Plasmids

The plasmids pON/C-5B/KE (Fig. 1a) and pHCV-O were described previously [Ikeda et al., 2005]. This plasmid includes the adaptive mutation of K1609E of NS3 to enhance the efficiency of replication, this adaptive mutation was reported by Lohman et al. (22) The plasmid pON/C-5B/KE contains neomycin phosphotransferase (Neo) downstream of HCV IRES and the full length HCV-O polyprotein coding sequence downstream of encephalomyocarditis virus (EMCV) IRES. To introduce a pON/C-5B/KE/(V85I), pON/C-5B/KE/(K124E), pON/C-5B/KE/(V85I&K124E), we first made PCR fragments including the partial NS5B region with the primers 5′-ggatcccgatctcagcgacgg-3′ and 5′-tctagaggtcccattcgccattac-3′. This 2.4-kb fragment was subcloned into pSTBlue1 Blunt vector (Novagen, Madison, WI) to generate pSTBlue-1MN002. Each vector expressing the V85I mutant, K124E mutant, and V85I&K124E double mutant of HCV-O was generated by Quick Change mutagenesis (Stratagene, La Jolla, CA) to generate pSTBlueMN002(V85I), pSTBlueMN002(K124E) pSTBlueMN002(V85I&K124E). Next, pON/C-5B was

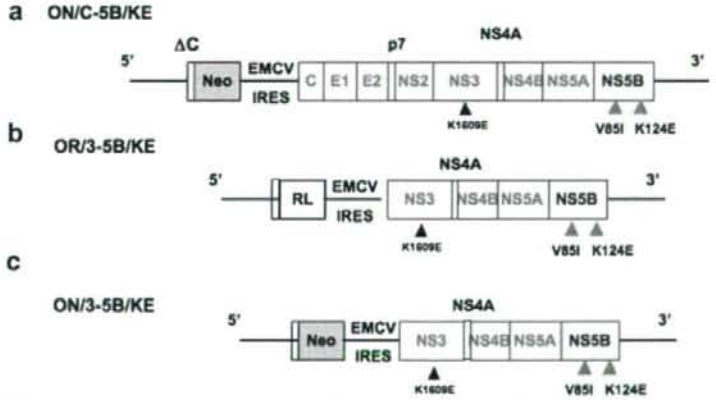

Fig. 1. **a**: Organization of genome-length HCV RNA derived from HCV-O. Open reading frames, untranslated regions, EMCV IRES, and Neo genes are depicted as shaded boxes, thin lines, thick lines, and open boxes, respectively. ΔC indicates the 12 N-terminal amino acid residues of the core as a part of IRES. This construct also contains adaptive mutation K1609E which is indicated by a black triangle. We use this construct as a wild type. Grey triangle is the position of 85 and 124 in NS5B which we generated mutation to the replicon for this experiments. **b**: The construct of the reporter subgenomic HCV replicon carries the renilla luciferase gene (RL). **c**: The construct of the reporter subgenomic HCV replicon carries the Neo gene.

digested with *Sna*b1 and *Xba*1 and subcloned into pSTBlue-1 to create pSTBlueMN001. All of the pSTBlue-MN002mutants were digested with *Bam*H1 and *Xba*1, which were subcloned into pSTBlueMN001 to create pSTBlueMN001mutant. The pSTBlueMN001 mutants were digested with *Sna*b1 and *Xba*1 and re-ligated in pON/C-5B/KE to introduce pON/C-5B/KE/(V85I), pON/C-5B/KE/(K124E), pON/C-5B/(V85I&K124E). The plasmids pOR/3-5B/KE/(V85I), pOR/3-5B/KE/(K124E) and pOR/3-5B/KE/(V85I&K124E), were constructed from pOR/3-5B/KE (Fig. 1b) by swapping for fragments of pSTBlueMN001 mutants digested with *Sna*b1 and *Xba*1. DNA sequencing of the manipulated regions of the plasmids verified all mutations.

RNA Transfection and Selection of G418-Resistant Cells

For electroporation, OR6c cells were washed twice with ice-cold phosphate buffered saline (PBS) and resuspended at 10^7 cells/ml in PBS. Twenty microgram of ON/C-5B/KE or its mutant derived RNA was mixed with 500 μl of the cell suspension in a cuvette with a gap width of 0.2 cm (Bio-Rad, Hercules, CA). The mixture was immediately subjected to two pulses of current at 1.2 kV, 25 μF, and maximum resistance. Following 10 min of incubation at room temperature, cells were seeded into 10-cm dishes. Cells were selected in complete DMEM with 300 μg/ml G418. About 3 weeks after transfection and G418 selection, cells were fixed and stained with Coomassie brilliant blue (0.6 g/l in 50% methanol–10% acetic acid) and the number of colonies was counted.

Transient-Replication Assays With Luciferase Replicons

OR6c cells were transfected by electroporation as the same protocol described above using 20 μg of OR/3-5B/KE or its mutants derived RNAs carrying the renilla luciferase (RL) gene. After addition of 2 ml of complete DMEM, 2×10^4 of aliquot OR6c cells were plated in 24-well plates at least in triplicate for each assay and harvested at various time points with renilla lysis reagent (Promega KK, Tokyo, Japan) and subjected to the RL assay according to the manufacturer's protocol (Promega). Values obtained with cells harvested 6 hr after electroporation were used to correct for the transfection efficiency.

IFN and Ribavirin Treatment

To monitor the anti-HCV effect of IFN and RBV on replication, OR6c cells were transfected by electroporation using 10 μg of OR/3-5B/KE derived RNAs as described elsewhere [Crotty et al., 2000]. OR6c cells (2×10^4/well) were plated onto 24-well plates at least in triplicate for each assay and cultured for 4 hr. Then the cells were treated with IFN at a final concentration of 1, 2, 4, 10, and 20 units/ml or RBV at a final concentration of 50,100, and 200 μM for 72 hr, harvested with renilla lysis reagent (Promega), and assayed for luciferase activity according to the manufacturer's protocol. We also studied about the additional effect of RBV (100 μM) on IFN (1 u/ml).

Cell Viability

We checked toxic effect of IFN and RBV. Effect of IFN (1 and 4 units/ml), and RBV (50 and 100 μM) on cell viability was investigated. To examine the cytotoxic effect of IFN and RBV on OR6c cells with OR/3-5B/KE replicon RNA, the cells were seeded at a density of 2×10^5 cells per dish onto 6-well plates. After 24-hr culture, the cells were treated with IFN or RBV at final concentrations of 2 and 4 units/ml or 50 and 100 μM, respectively, in the absence of G418. After incubation for 72 hr, the number of viable cells was counted in an improved Neubauer-type hemocytometer after trypan blue dye (Invitrogen) treatment.

Indirect Immunofluorescence

Cells were grown on four-well chamber slides until 70–80% confluent, washed three times with PBS, and fixed in methanol–acetone (1:1, v/v) for 10 min at room temperature. Dilutions of primary murine monoclonal antibody to residues 21–40 of the core protein (2Zcp11; Tokushu Men-eki Institute, Tokyo) (1:1,000), were prepared in PBS containing 3% bovine serum albumin and incubated with fixed cells for 2 hr at room temperature. After additional washes with PBS, specific antibody binding was detected with a goat anti-mouse immunoglobulin G-fluorescein isothiocyanate-conjugated secondary antibody (Jackson ImmunoResearch, West Grove, PA) diluted 1:500. Cells were washed with PBS, and mounted in DAKO Fluorescent mounting medium (DAKO Japan, Tokyo, Japan) prior to examination using a Zeiss AxioPlan2 fluorescence microscope.

Statistical Analysis

Difference in relative luciferase activity among mutant replicons and differences in anti-HCV activity of RBV among mutant replicons were tested using Student's *t*-test and Mann–Whitney *U*-test as appropriate. *P*-values <0.05 were considered statistically significant.

RESULTS

Mutation in NS5B Enhances Levels of Replication on Transient Assay

To investigate whether the mutations in NS5B of the HCV genome affect replication, we used subgenomic HCV replicons with the renilla luciferase gene for transient assay [Ikeda et al., 2005]. In a previous study [Kumagai et al., 2004], substitution of glutamic acid at the 124th position with lysine and substitution of isoleucine at the 85th position with valine in NS5B yielded a complete match with the population of good

responders (5 out of 5 patients). We introduced mutations to two different types of replicon to obtain ON/C-5B/KE(V85I), ON/C-5B/KE/(K124E), ON/C-5B/KE (V85I&K124E), OR/3-5B/KE/(V85I), OR/3-5B/KE(K124E), and OR/3-5B/KE(V85I&K124E) as described in Materials and Methods Section. The subgenomic replicons with V85I showed higher replication activity than the wild-type replicon in OR6c cells (Fig. 2). Also the replicon with K124E and the replicon with V85I&K124E showed slightly higher replication activity than the wild type, but the replicon with K124E single amino acid mutation did not show statistically higher replication activity than the wild type (Fig. 2). We initially expected that double mutations (V85I&K124E) would lead to better replication than either of the single mutations (V85I or K124E), but interestingly the V85I mutation on NS5B replicated best. This result indicated that the level of replication was affected by amino acid substitution at the 85th position.

Mutation in NS5B Enhances the Efficiency of Colony Formation in Cured Cells

In colony formation assay, we used cured subgenomic replicon cells (OR6c), since cured cells enhanced colony formation of the replicon more efficiently than did parental HuH-7 cells. We examined the effect of these mutations in full-length replicon, ON/C-5B/KE by a colony formation assay. In the initial experiment, we introduced each 20 μg of RNA derived from the ON/C-5B/KE, ON/C-5B/KE/(V85I), ON/C-5B/KE/(K124E), and ON/C-5B/KE/(V85I&K124E) into OR6c cells. After 3 weeks of G418 selection at a concentration of 300 μg/ml, only one colony was obtained and the same result was obtained with ON/C-5B/KE(K124E) and ON/C-5B/KE/(V85I&K124E) transcripts. In repeated experiments, the number of G418-resistant colonies was reproducibly one or zero, but when ON/C-5B/KE/(V85I) transcripts was electroporated, G418 resistant 4–6 colonies was obtained in repeated experiments. These results also confirm that the replication level of ON/C-5B//KE/(V85I) is higher than that of ON/C-5B/KE, ON/C-5B/KE/(K124E) and ON/C-5B/KE/(V85I&K124E).

As the efficiency of colony formation with full-length replicon (ON/C-5B/KE; Fig. 1a) was quite low, we investigated colony formation with subgenomic replicon, ON/3-5B/KE (Fig. 1c). Figure 3 shows the representative result of three independent colony formation assays. The efficiency of colony formation of ON/3-5B/KE was better than that of full-length replicon and the colony formation of in vitro transcript of ON/3-5B/KE, ON/3-5B//KE/(V85I), ON/3-5B/KE/(K124E) and ON/3-5B/KE/(V85I&K124E) was 39 (61), 157 (132), 44 (54), and 134 (107), respectively (the numbers in parentheses show another set of result). The efficiency of colony formation of ON/3-5B//KE/(V85I) was greater than that of ON/C-5B/KE and it showed a similar result with that obtained from genome-length replicon.

Inhibition of HCV RNA Replication by IFN and RBV

We examined the inhibitory effect of IFN and RBV on the replication of OR/3-5B/KE. In this experiment, the subgenomic replicon system was used. OR6c cells were treated with IFN at concentrations of 1–20 μM (Fig. 4) and RBV at concentrations of 50, 100, and 200 μM (Fig. 5) after transfection of OR/3-5B/KE derived RNA. Since it is important to know how IFN and RBV treatment is toxic to the cells, we examined cell viability after treatment with 50 and 100 μM of RBV or 2 and 4 units/ml of IFN. The cell viability of OR6c was not

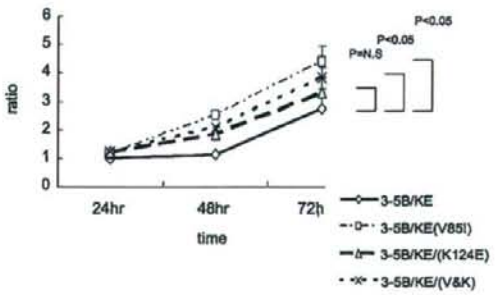

Fig. 2. Effect of amino acid substitutions in NS5B on transient replication activity of replicon. The replication activity of reporter subgenomic HCV replicon with mutation of V85I, K124E, or V85I and K124E (V&K) was compared with that of wild-type in OR6c cells (transient transfection). After 72 hr of transfection, the Renilla luciferase (RL) assay was performed as described in the Materials and Methods section. The relative RL activity (ratio) of mutants was calculated in comparison to that of subgenomic replicon of wild-type (assigned as 1). The data indicate means ± SD of triplicates from three independent experiments. 3-5B/KE: OR/3-5B/KE, 3-5B/KE(V85I): OR/3-5B(K124E), 3-5B/KE/(K124E): OR3-5B/KE/(K124E), 3-5B/KE/(V&K): OR/3-5B/KE/(V85I&K124E).

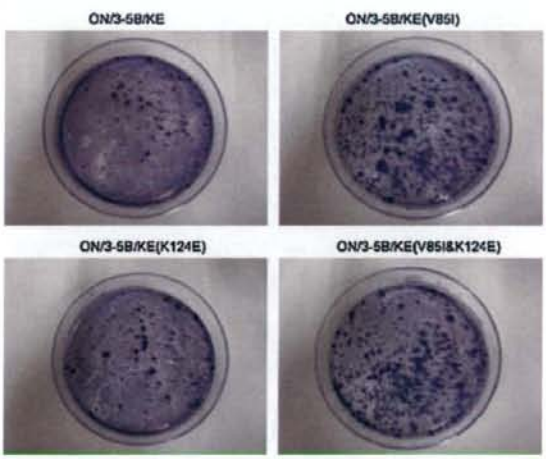

Fig. 3. Colony formation assay of OR6c cells transfected with wild-type and three different mutant replicons. A representative result of colony formation assay using subgenomic replicon RNA (ON/3-5B/KE) system. The efficacy of colony formation was much higher than that of full-length replicon RNA (ON/C-5B/KE). In this series of photographs, colony forming unit of ON/3-5B/KE, ON/3-5B//KE/(V85I), ON/3-5B/KE/(K124E) and ON/3-5B/KE/(V85I&K124E) was 2.7/μg, 6.7/μg, 3.0/μg and 5.4/μg, respectively.

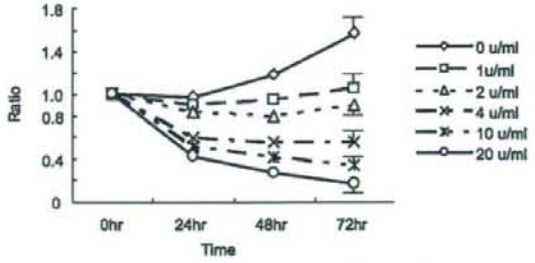

Fig. 4. Dose-dependent inhibition of replication by interferon-α (IFN). OR6 cells were transfected with wild-type replicon (OR/3-5B/KE). Inhibition of HCV RNA replication in the OR6c cell treated with IFN-α was shown at the indicated time (24, 48, and 72 hr) from the start of treatment. The cells were treated with IFN-α (0, 1, 2, 4, 10, and 20 u/ml), and the Renilla luciferase assay was performed as described in Materials and Methods Section. The relative luciferase activity (%) calculated at each point, where the luciferase activity of non-treated cells at 0 hr was assigned to be 100%, is presented. The data indicate means ± SD of triplicates from three independent experiments.

changed by these treatments (Fig. 6), indicating that both IFN and RBV were not toxic to the cells at the indicated concentrations. As shown in Figures 4 and 5, the inhibition of HCV RNA replication occurred in a dose-dependent manner with IFN or RBV treatments. RBV at a concentration of 100 μM inhibited replication of RNA (Fig. 5), but was not toxic to OR6c cells (Fig. 6).

The inhibitory effect of 100 μM RBV on RNA replication in each mutant was also examined. Various biological effect of IFN has been investigated and its effect on cell cycle or cell-differentiation is strong, and we focused on the effect of mutants on RBV treatment. To see this effect, we compared between IFN alone and IFN + RBV. As shown in Figure 7, no difference between three mutants was seen in the treatment with 1 unit/ml of IFN. The proliferation of each mutant RNA was similarly reduced to around a ratio of 0.6. On the other hand, addition of 100 μM of RBV was differently affected by each mutation pattern (Fig. 8). The single mutant with V85I and double mutants with V85I and K124E

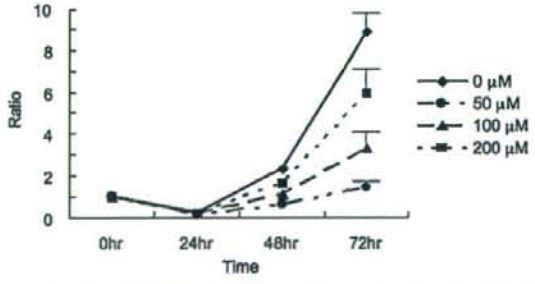

Fig. 5. Dose-dependent inhibition of HCV RNA replication by ribavirin. OR6 cells were transfected with wild-type replicon (OR/3-5B/KE) and treated with ribavirin at concentrations of 50, 100, and 200 μM for 72 hr. Inhibition of HCV RNA replication in the OR6c cell treated with ribavirin (RBV) was shown at the indicated time (24, 48, and 72 hr) from the start of treatment. The relative luciferase activity (%) calculated at each point, where the luciferase activity of non-treated cells at 0 hr was assigned to be 100%, is presented. The data indicate means ± SD of triplicates from three independent experiments.

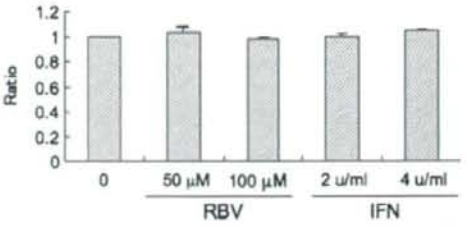

Fig. 6. Cytotoxicity of ribavirin (RBV) or interferon-α (IFN) on replicon RNA in OR6c cells. OR6c cells with OR/3-5B/KE RNA were cultured in the absence or presence of RBV or IFN (50 and 100 μM or 2 and 4 u/ml) for 72 hr, and then the cell viability was determined as described in Materials and Methods Section. The relative cell viability (%) calculated at each point, when viability of non-treated cells was assigned to be 100%, is presented. The data indicate means ± SD of triplicates from three independent experiments.

were significantly increased in RNA proliferation. The degree of inhibition by RBV in OR/3-5B/KE(V85I) and OR/3-5B/KE(V85I&K124E) was significantly lower than that in OR/3-5B/KE, although the difference of OR/3-5B/KE(K124E) was not significant.

Indirect Immunofluorescence

To confirm the presence of replicating full-length RNAs in cells selected for G418 resistance following transfection with ON/C-5B/KE(V85I), one G418-resistant cell colony was selected at random and clonally cultured. We confirmed HCV protein expression by indirect immunofluorescence imaging and observed core protein in the replicon cells (OR6) (Fig. 9c), HCV core protein was demonstrated in the clonally isolated cell line selected after transfection with ON/C-5B/KE(V85I)

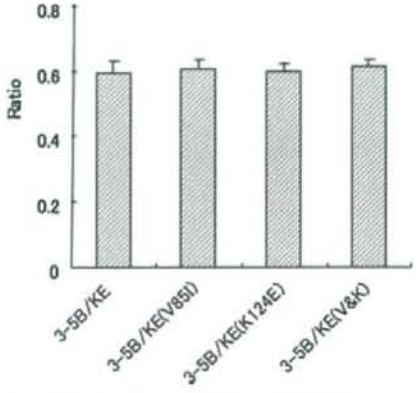

Fig. 7. Effect of interferon-α (IFN) on the subgenomic HCV replicon possessing the Renilla luciferase reporter. The replication levels of the subgenomic HCV replicons were monitored by luciferase reporter assay with IFN 0 u/ml or IFN 1 u/ml for 72 hr. Renilla luciferase assay was performed as described in Materials and Methods Section. The relative luciferase unit with IFN (1 u/ml) treatment were calculated, where the luciferase unit without IFN treatment was assigned to be 1, and compared between wild type (OR/3-5B/KE) and other three mutants (OR/3-5B/KE(V85I), OR/3-5B/KE(K124E), OR/3-5B/KE(V&K)). The data indicate means ± SD of triplicates from two independent experiments.

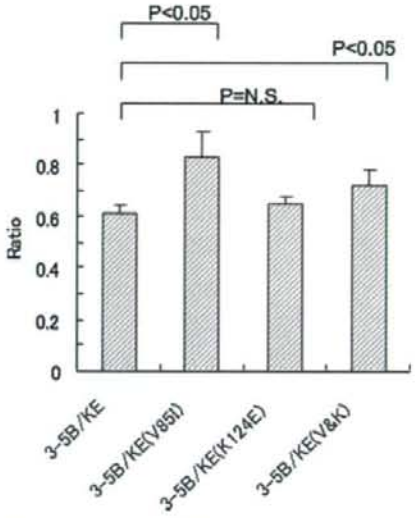

Fig. 8. Effect of interferon-α (IFN) and ribavirin (RBV) combination treatment on the replication levels of the subgenomic HCV replicon possessing the Renilla luciferase reporter. The replication levels of the subgenomic HCV replicons were monitored by luciferase reporter assay with IFN 1 u/ml or IFN 1 u/ml and ribavirin 100 μM for 72 hr. The relative luciferase unit of IFN 1 u/ml and ribavirin 100 mM treatment were calculated, where the luciferase unit of IFN 1 u/ml treatment was assigned to be 1, and compared in wild type (OR/3-5B/KE) and other three mutants (OR/3-5B/KE(V85I), OR/3-5B/KE(K124E), OR/3-5B/KE(V&K)). The data indicate means ± SD of triplicates from three independent experiments.

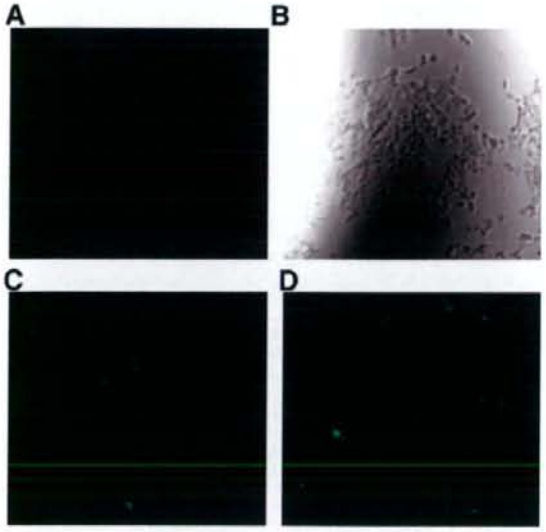

Fig. 9. Indirect immunofluorescence detection of HCV core antigen in normal OR6c cells (cured cell) (**a**), OR6 cells (wild-type HCV replicon) (**c**), and a clonally isolated cell line selected following transfection of OR6c cells with ON/3-5B/V85I (cell line 1) (**d**) and the correspondent phase-contrast microscopic photograph of OR6c cells (**b**).

(Fig. 9d), while it was not observed in the cured cell line (OR6C) (Fig. 9a,b).

DISCUSSION

Predictive factors for a sustained viral response (SVR) in IFN monotherapy or combination therapy have been vigorously investigated in prior studies. In addition to several host and viral factors, such as HCV genotypes, baseline viral load, stage of fibrosis, gender, age, and obesity [Saito et al., 2000, 2006], disappearance of serum HCV RNA during the early phase of therapy or a rapid decrease in HCV RNA levels are significant factors for achieving a SVR [Ferenci et al., 2001]. In our previous study, two distinct amino acid substitutions in the NS5B region of the HCV genome correlated with early viral responses in combination therapy [Kumagai et al., 2004]. NS5B of the HCV genome codes for RdRP, which regulates viral replication. Thus, the detected mutations might increase replication efficacy of HCV or induce resistance to the anti-viral effect of RBV, which could lead to resistance to therapy in the early phase. It was thought that the HCV replicon system would be a good tool for examining the correlation between viral mutation and replication capability. One of the mutation-introduced replicons (V85I) showed a higher replication activity than that of the wild type, and, consistent with our previous clinical study, this mutant was resistant to in vitro RBV treatment. The present study is the first to examine the precise relationship between such mutations and clinical data on the early clearance of HCV during IFN and RBV combination therapy. The mutations of V85I and K124E in NS5B have never been reported in the replicon system.

We investigated the effect of both IFN and RBV on the wild type and three mutants in NS5B at non-toxic concentration to the host cell (Fig. 6). One unit of IFN did not affect the replication of mutants (Fig. 7) but RBV significantly affected the replication of three mutants in the presence of IFN (Fig. 8). These results indicated that the polymorphism of NS5B affect sensitivity to RBV treatment. Although it has been known in the clinical setting that HCV RNA levels are not changed in patients with chronic hepatitis C during RBV monotherapy, our in vitro results showed the reduction of HCV RNA replication with RBV treatment. It was reported that serum levels of RBV in patients with chronic hepatitis C under IFN + RBV combination therapy was very low such as 10^{-14} mM [Naka et al., 2005], however, we can examine the anti-viral effect of much higher levels of RBV on the replicon system without a direct toxic effect of RBV in HuH7 cells. The possibility of a difference between circulating HCV particles and the replicon system in terms of RBV sensitivity may still exist, but this question will be further investigated using a recently developed cell culture system.

We used a dicistronic genome length and subgenome HCV RNA replication systems, which were established previously using HCV RNA from HCV-O infected in non-neoplastic human hepatocyte PH5CH8 cells. For the

cells into which genome-length and subgenomic HCV RNA were introduced, we chose the cloned cell line OR6c, prepared by IFN treatment from subgenomic HCV replicon-supporting cells, since OR6c had a higher efficiency of colony formation (ECF) than its parental HuH-7 cell line in a study of subgenomic HCV replicons [Blight et al., 2002]. It is known that the efficiency of colony formation is unstable, so that the luciferase activity and the colony-forming unit are always discrepant. The impact of ON/C-5B/KE(V85I) on colony formation was about 4 times that of the wild-type replicon in genome length and subgenomic RNAs, and the V85I mutation in NS5B showed 1.5 times higher replication activity in luciferase assay than the wild type in the subgenomic replicon system. Young et al. reported an RBV-resistant NS5B mutation during RBV monotherapy [Young et al., 2003], but this phenylalanine to tyrosine amino acid substitution located at the 415th position in NS5B differed from our amino acid substitution. Replicon cells were selected after G418 exposure, and the replication may be amplified by this selection culture. We sequenced the NS5B region, which includes the 85th and 124th nucleotide portions, from some clones 2 months after G418 selection culture, and we did not found significant mutations. From the present in vitro study and previous clinical study, it may be concluded that at least V85I mutation in NS5B increases viral replication that may cause resistance to RBV treatment.

Two of the patients in the clinical study [Kumagai et al., 2004] had previously been treated with IFN-α monotherapy in our previous study: one patient (Pt 3) has V85 and K124 in the HCV RdRP and the other (Pt 7) had I85 and E124. The former was a good responder to IFN-α and RBV combination therapy, but the latter was not. This result indicated that I85V and E124K substitutions did not affect the response to IFN-α monotherapy, because both types had failed to respond previously to IFN monotherapy. Therefore, we surmised that this amino acid substitution influenced the response to RBV anti-viral activity, which prompted us to examine the effect of RBV on viral replication. Several mechanisms of anti-viral activity of RBV have been proposed [Tam et al., 1999; Maag et al., 2001; Lau et al., 2002], but it is unclear why only the V85I single amino acid substitution induced replication better than the wild type. As shown previously [Kumagai et al., 2004], the 85th amino acid of HCV RdRP is distant from the active site of polymerase but is located near the RNA primer binding site, and this substitution may influence nucleotide misincorporation during polymerization. This 85th position is more important than the 124th position for replication of HCV-O.

This study is the first to examine whether NS5B polymorphism affects the replication efficiency and anti-HCV effect of RBV in an HCV RNA replicon system. It will be interesting to know whether these mutations in other genotypes (genotypes 2 and 3) replicate more efficiently and are more resistant than genotype 1b to RBV alone. Our data suggested that during clinical use of RBV, several mutations in the HCV genome might occur, such as in the isoleucine residue at the 85th position of HCV NS5B, which then affect viral replication and RBV resistance. This viral mutation may be one of the reasons for the failure in early viral clearance by IFN and RBV. There are, however, many factors that influence the success of IFN and RBV combination therapy. The resistance or sensitivity to IFN or peg-IFN, not to RBV, might also affect the early viral response, and many factors in both viral and host sides are known to affect IFN responsiveness, such as NS5A mutations [Enomoto et al., 1996], immunological status [Saito et al., 2000], or irf-1 gene promoter polymorphisms [Saito et al., 2002, 2005]. Together, these factors might determine the efficacy of anti-viral therapy in vivo, and the present in vitro data provides evidence partially supporting our clinical observations that NS5B polymorphisms are associated with early viral clearance during IFN and RBV therapy. However, it is unclear whether this single mutation occurs with peg-IFN plus RBV combination therapy and further studies are necessary. Nevertheless, our report is useful for modeling targets for antiviral compounds for the treatment of HCV.

REFERENCES

Blight KJ, McKeating JA, Rice CM. 2002. Highly permissive cell lines for subgenomic and genomic hepatitis C virus RNA replication. J Virol 76:13001–13014.

Bouvier-Alias M, Patel K, Dahari H, Beaucourt S, Larderie P, Blatt L, Hezode C, Picchio G, Dhumeaux D, Neumann AU, McHutchison JG, Pawlotsky JM. 2002. Clinical utility of total HCV core antigen quantification: A new indirect marker of HCV replication. Hepatology 36:211–218.

Contreras AM, Hiasa Y, He W, Terella A, Schmidt EV, Chung RT. 2002. Viral RNA mutations are region specific and increased by ribavirin in a full-length hepatitis C virus replication system. J Virol 76: 8505–8517.

Crotty S, Maag D, Arnold JJ, Zhong W, Lau JY, Hong Z, Andino R, Cameron CE. 2000. The broad-spectrum antiviral ribonucleoside ribavirin is an RNA virus mutagen. Nat Med 6:1375–1379.

Enomoto N, Sakuma I, Asahina Y, Kurosaki M, Murakami T, Yamamoto C, Ogura Y, Izumi N, Marumo F, Sato C. 1996. Mutations in the nonstructural protein 5A gene and response to interferon in patients with chronic hepatitis C virus 1b infection. N Engl J Med 334:77–81.

Feld JJ, Hoofnagle JH. 2005. Mechanism of action of interferon and ribavirin in treatment of hepatitis C. Nature 436:967–972.

Ferenci P, Brunner H, Nachbaur K, Datz C, Gschwantler M, Hofer H, Stauber R, Hackl F, Jessner W, Rosenbeiger M, Munda-Steindl P, Hegenbarth K, Gangl A, Vogel W. 2001. Combination of interferon induction therapy and ribavirin in chronic hepatitis C. Hepatology 34:1006–1011.

Fried MW, Shiffman ML, Reddy KR, Smith C, Marinos G, Goncales FL, Jr., Haussinger D, Diago M, Carosi G, Dhumeaux D, Craxi A, Lin A, Hoffman J, Yu J. 2002. Peginterferon alfa-2a plus ribavirin for chronic hepatitis C virus infection. N Engl J Med 347:975–982.

Gao B, Hong F, Radaeva S. 2004. Host factors and failure of interferon-alpha treatment in hepatitis C virus. Hepatology 39:880–890.

Ikeda M, Abe K, Dansako H, Nakamura T, Naka K, Kato N. 2005. Efficient replication of a full-length hepatitis C virus genome, strain O, in cell culture, and development of a luciferase reporter system. Biochem Biophys Res Commun 329:1350–1359.

Kumagai N, Takahashi N, Kinoshita M, Tsunematsu S, Tsuchimoto K, Saito H, Ishii H. 2004. Polymorphisms of NS5B protein relates to early clearance of hepatitis C virus by interferon plus ribavirin: A pilot study. J Viral Hepat 11:225–235.

Lanford RE, Guerra B, Lee H, Averett DR, Pfeiffer B, Chavez D, Notvall L, Bigger C. 2003. Antiviral effect and virus-host

interactions in response to alpha interferon, gamma interferon, poly(i)-poly(c), tumor necrosis factor alpha, and ribavirin in hepatitis C virus subgenomic replicons. J Virol 77:1092–1104.

Lau JY, Tam RC, Liang TJ, Hong Z. 2002. Mechanism of action of ribavirin in the combination treatment of chronic HCV infection. Hepatology 35:1002–1009.

Liang TJ, Rehermann B, Seeff LB, Hoofnagle JH. 2000. Pathogenesis, natural history, treatment, and prevention of hepatitis C. Ann Intern Med 132:296–305.

Lohmann V, Korner F, Dobierzewska A, Bartenschlager R. 2001. Mutations in hepatitis C virus RNAs conferring cell culture adaptation. J Virol 75:1437–1449.

Lukasiewicz E, Hellstrand K, Westin J, Ferrari C, Neumann AU, Pawlotsky JM, Schalm SW, Zeuzem S, Veldt BJ, Hansen BE, Verhey-Hart E, Lagging M. 2007. Predicting treatment outcome following 24 weeks peginterferon alpha-2a/ribavirin therapy in patients infected with HCV genotype 1: Utility of HCV-RNA at day 0, day 22, day 29, and week 6. Hepatology 45:258–259.

Maag D, Castro C, Hong Z, Cameron CE. 2001. Hepatitis C virus RNA-dependent RNA polymerase (NS5B) as a mediator of the antiviral activity of ribavirin. J Biol Chem 276:46094–46098.

Manns MP, McHutchison JG, Gordon SC, Rustgi VK, Shiffman M, Reindollar R, Goodman ZD, Koury K, Ling M, Albrecht JK. 2001. Peginterferon alfa-2b plus ribavirin compared with interferon alfa-2b plus ribavirin for initial treatment of chronic hepatitis C: A randomised trial. Lancet 358:958–965.

Naka K, Ikeda M, Abe K, Dansako H, Kato N. 2005. Mizoribine inhibits hepatitis C virus RNA replication: Effect of combination with interferon-α. Biochem Biophys Res Commun 330:871–879.

Pol S, Nalpas B, Bourliere M, Couzigou P, Tran A, Abergel A, Zarski JP, Berthelot P, Brechot C. 2000. Combination of ribavirin and interferon-alfa surpasses high doses of interferon-alfa alone in patients with genotype-1b-related chronic hepatitis C. Hepatology 31:1338–1344.

Poynard T, McHutchison J, Goodman Z, Ling MH, Albrecht J. 2000. Is an "a la carte" combination interferon alfa-2b plus ribavirin regimen possible for the first line treatment in patients with chronic hepatitis C? The ALGOVIRC Project Group. Hepatology 31:211–218.

Saito H, Ebinuma H, Satoh I, Miyaguchi S, Tada S, Iwabuchi N, Kumagai N, Tsuchimoto K, Morizane T, Ishii H. 2000. Immunological and virological predictors of outcome during interferon-alpha therapy of chronic hepatitis C. J Viral Hepat 7:64–74.

Saito H, Tada S, Wakabayashi K, Nakamoto N, Takahashi M, Nakamura M, Ebinuma H, Ishii H. 2002. The detection of IRF-1 promoter polymorphisms and their possible contribution to T helper 1 response in chronic hepatitis C. J Interferon Cytokine Res 22: 693–700.

Saito H, Tada S, Nakamoto N, Kitamura K, Horikawa H, Kurita S, Ebinuma H, Ishii H, Takahashi M, Tanaka S, Hibi T. 2005. Contribution of Irf-1 promoter polymorphisms to the Th1-type cell response and interferon-beta monotherapy for chronic hepatitis C. Hepatol Res 32:25–32.

Saito H, Tada S, Ebinuma H, Ishii H, Kashiwazaki K, Takahashi M, Tsukada N, Nishida J, Tanaka S, Shiozaki H, Hibi T. 2006. Role of erythrocytes as a reservoir for ribavirin and relationship with adverse reactions in the early phase of interferon combination therapy for chronic hepatitis C virus infections. J Clin Microbiol 44: 3562–3568.

Saracco G, Ciancio A, Olivero A, Smedile A, Roffi L, Croce G, Colletta C, Cariti G, Andreoni M, Biglino A, Calleri G, Maggi G, Tappero GF, Orsi PG, Terreni N, Macor A, Di Napoli A, Rinaldi E, Ciccone G, Rizzetto M. 2001. A randomized 4-arm multicenter study of interferon alfa-2b plus ribavirin in the treatment of patients with chronic hepatitis C not responding to interferon alone. Hepatology 34:133–138.

Sidwell RW, Huffman JH, Khare GP, Allen LB, Witkowski JT, Robins RK. 1972. Broad-spectrum antiviral activity of Virazole: 1-beta-D-ribofuranosyl-1,2,4-triazole-3-carboxamide. Science 177:705–706.

Takahashi M, Saito H, Higashimoto M, Atsukawa K, Ishii H. 2005. Benefit of hepatitis C virus core antigen assay in prediction of therapeutic response to interferon and ribavirin combination therapy. J Clin Microbiol 43:186–191.

Tam RC, Pai B, Bard J, Lim C, Averett DR, Phan UT, Milovanovic T. 1999. Ribavirin polarizes human T cell responses towards a Type 1 cytokine profile. J Hepatol 30:376–382.

Young KC, Lindsay KL, Lee KJ, Liu WC, He JW, Milstein SL, Lai MM. 2003. Identification of a ribavirin-resistant NS5B mutation of hepatitis C virus during ribavirin monotherapy. Hepatology 38: 869–878.

Zeuzem S, Lee JH, Franke A, Ruster B, Prummer O, Herrmann G, Roth WK. 1998. Quantification of the initial decline of serum hepatitis C virus RNA and response to interferon alfa. Hepatology 27:1149–1156.

Research Article

The Polycomb Gene Product BMI1 Contributes to the Maintenance of Tumor-Initiating Side Population Cells in Hepatocellular Carcinoma

Tetsuhiro Chiba,[1,4] Satoru Miyagi,[1] Atsunori Saraya,[1] Ryutaro Aoki,[1] Atsuyoshi Seki,[1] Yohei Morita,[3] Yutaka Yonemitsu,[2] Osamu Yokosuka,[2] Hideki Taniguchi,[5] Hiromitsu Nakauchi,[3] and Atsushi Iwama[1,4]

[1]Department of Cellular and Molecular Medicine and [2]Department of Medicine and Clinical Oncology, Graduate School of Medicine, Chiba University, Chiba, Japan; [3]Laboratory of Stem Cell Therapy, Center for Experimental Medicine, University of Tokyo; [4]JST, CREST, Tokyo, Japan; and [5]Department of Regenerative Medicine, Graduate School of Medical Science, Yokohama City University, Yokohama, Japan

Abstract

Side population (SP) cell analysis and sorting have been successfully applied to hepatocellular carcinoma (HCC) cell lines to identify a minor cell population with cancer stem cell properties. However, the molecular mechanisms operating in SP cells remain unclear. The polycomb gene product BMI1 plays a central role in the self-renewal of somatic stem cells in a variety of tissues and organs and seems to be implicated in tumor development. In this study, we determined the critical role of BMI1 in the maintenance of cancer stem cells with the SP phenotype in HCC cell lines. BMI1 was preferentially expressed in SP cells in Huh7 and PLC/PRF/5 HCC cells compared with the corresponding non-SP cells. Lentiviral knockdown of *BMI1* considerably decreased the number of SP cells in both Huh7 and PLC/PRF/5 cells. Long-term culture of purified SP cells resulted in a drastic reduction in the SP subpopulation upon the *BMI1* knockdown, indicating that BMI1 is required for the self-renewal of SP cells in culture. More importantly, the *BMI1* knockdown abolished the tumor-initiating ability of SP cells in nonobese diabetic/severe combined immunodeficiency mice. Derepression of the *INK4A* and *ARF* genes that are major targets for BMI1 was not necessarily associated with impaired self-renewal of SP cells caused by *BMI1* knockdown. In conclusion, our findings define an important role for BMI1 in the maintenance of tumor-initiating SP cells in HCC. BMI1 might be a novel therapeutic target for the eradication of cancer stem cells in HCC. [Cancer Res 2008;68(19):7742–9]

Introduction

According to the recent "cancer stem cell hypothesis," tumors consist of a minor component of tumorigenic cells and a major component of nontumorigenic cells (1, 2). The minor population, termed cancer stem cells or tumor-initiating cells, construct a hierarchical structure containing varied descendants in a similar fashion to the normal stem cell systems and possesses a prominent ability to initiate new tumors in xenograft transplantation (3, 4). In addition, these cells seem to be highly resistant to traditional forms of anticancer therapy such as chemotherapy and radiotherapy (5, 6), resulting in residual cancer stem cells which, in many instances, lead to the recurrence of the cancer (7). Therefore, an overall understanding of the various biological aspects of cancer stem cells is of paramount importance to both the elucidation of mechanisms underlying carcinogenesis and the establishment of novel therapeutic strategies.

Side population (SP) cell analysis and sorting were initially used for the isolation of hematopoietic stem cells in bone marrow cells (8). Currently, they are widely applied to the enrichment of putative normal stem cells in a variety of tissues and organs (9–11). The SP phenotype is determined by the ability to efflux the Hoechst 33342 dye through an ATP-binding cassette (ABC) membrane transporter. Of note, recent studies showed that SP cells isolated from diverse cancer cell lines harbor stem cell–like properties (12–14). Given that many different types of cancer cells frequently show overexpression of ABC transporters and exhibit drug resistance (15), it is quite reasonable to detect stem-like fractions in cancer cells using this approach. We previously applied SP analysis and sorting to established hepatocellular carcinoma (HCC) cell lines and found that in Huh7 and PLC/PRF/5 cells, SP fractions made up <1% of the total cell population (12). As expected, the SP subpopulations showed cancer stem cell–like properties both in culture and in an *in vivo* transplant model. These stem cell biology-based strategies enabled us to perform further analyses.

We and others previously reported that the polycomb-group (PcG) gene *Bmi1* plays a critical role in the self-renewal of a range of somatic stem cells, including hepatic stem cells, based on gain-of-function and loss-of-function analyses (16, 17). It seems likely that both normal and cancer stem cells share not only a number of surface marker phenotypes but also a list of molecular mechanisms for self-renewal and differentiation. This has been well shown in the leukemic stem cell system (18–20), although little is known in solid cancers.

In the current study, we examined the crucial role of BMI1 in the maintenance of the tumor-initiating SP subpopulation in HCC cells. Taking advantage of lentivirus-mediated knockdown and retrovirus-mediated overexpression techniques, we examined whether BMI1 regulates the self-renewal and differentiation of SP cells in culture and their tumorigenicity in a nonobese diabetic/severe combined immunodeficient (NOD/SCID) xenograft transplant model.

Note: Supplementary data for this article are available at Cancer Research Online (http://cancerres.aacrjournals.org/).

Requests for reprints: Atsushi Iwama, Department of Cellular and Molecular Medicine, Graduate School of Medicine, Chiba University, 1-8-1 Inohana, Chu-ku, Chiba 260-8670, Japan. Phone: 81-43-2262189; Fax: 81-43-2262191; E-mail: aiwama@faculty.chiba-u.jp.

doi:10.1158/0008-5472.CAN-07-5882

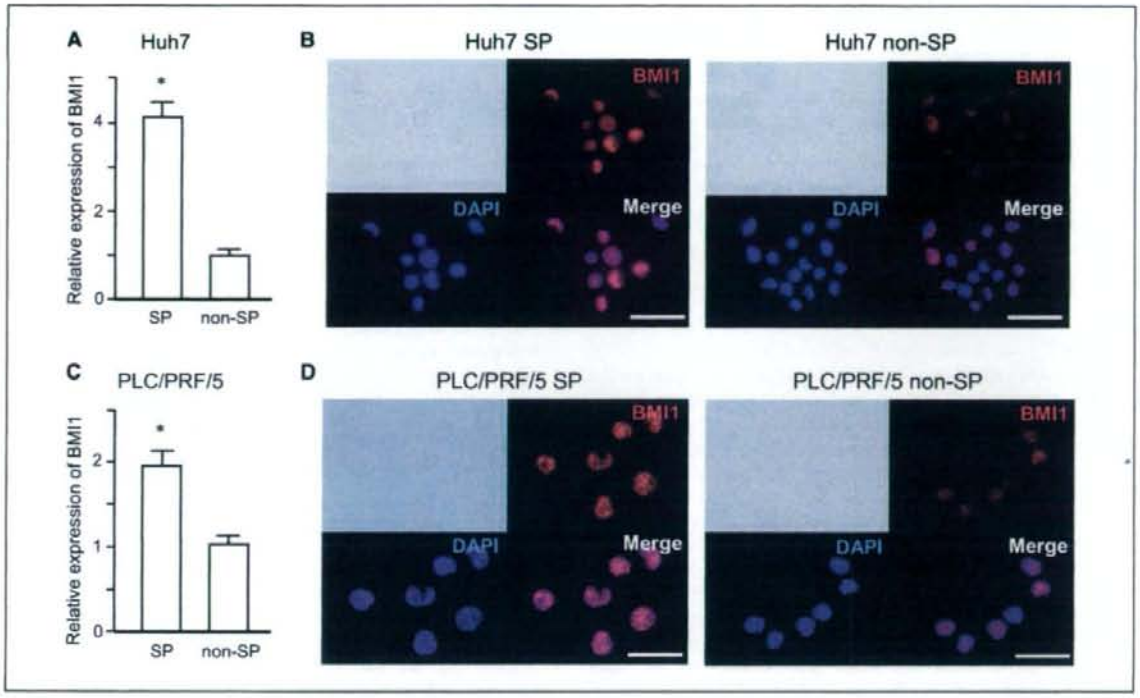

Figure 1. Expression of BMI1 in SP and non-SP cells. Real-time RT-PCR analyses of *BMI1* expression in SP and non-SP cells from Huh7 (*A*) and PLC/PRF/5 cells (*C*). Immunocytochemical analyses of BMI1 expression in SP and non-SP cells from Huh7 (*B*) and PLC/PRF/5 cells (*D*). Nuclear DAPI staining (*blue*) and immunofluorescent labeling of BMI1 (*red*) are merged. *, statistically significant ($P < 0.05$). *Scale bar*, 50 μm.

Materials and Methods

Mice. NOD/SCID mice were purchased from Sankyo Laboratory Co. Ltd. They were bred and maintained in accordance with our institutional guidelines for the use of laboratory animals.

Cell culture. The human liver cancer cell lines Huh7 and PLC/PRF/5 were cultured in DMEM (Invitrogen Life Technologies) containing 10% FCS and 1% penicillin/streptomycin (Invitrogen).

Flow cytometry. SP analysis and sorting were performed, as described previously (12). Briefly, the suspended cells were incubated at 37°C for 90 min with 20 μg/mL Hoechst 33342 (Sigma Chemical), either alone or in the presence of 50 μmol/L verapamil (Sigma). For the analysis of CD133 expression, cells were incubated with phycoerythrin-conjugated CD133/1 (Miltenyi Biotec). Propidium iodide (BD PharMingen) was added for the elimination of dead cells. Cell analysis and sorting were performed using MoFlo (DakoCytomation).

Immunocytochemistry. Freshly isolated SP cells and non-SP cells were placed on poly-L-lysine–coated slide glasses. After fixation with 2% paraformaldehyde and blocking in 10% goat serum, the cells were incubated with 0.5% Triton-X in PBS for 20 min at room temperature. After incubation, the cells were stained with a primary antibody, anti-Bmi1 (F6; Upstate Biotechnology), at a dilution of 1:200 for 12 h at 4°C. The cells then were washed and incubated with Alexa-555–conjugated goat anti-mouse IgG (Molecular Probes) at a dilution of 1:500 for 2 h at room temperature. After being washed in PBS, the cells were coverslipped with a mounting medium containing 4′,6-diamidino-2-phenylindole (DAPI; Vector Laboratories).

Viral production and transduction. Lentiviral vectors (CS-H1-shRNA-EF-1α-EGFP) expressing short hairpin RNA (shRNA) that targets human *BMI1* (target sequence: sh-*BMI1*-1, 5′-CAGATGAAGATAAGAGAAT-3′; sh-*BMI1*-2, 5′-GAGAAGGAATGGTCCACTT-3′) and *luciferase* were constructed. Human *BMI1* cDNA (a kind gift from Dr. Kazuhito Yamamoto) was cloned into a site upstream of IRES–enhanced green fluorescent protein (EGFP) in the pMCs-IG retroviral vector (21). Recombinant lentiviruses and retroviruses were produced as described before (17, 22).

Western blotting. Cells transduced with the indicated viruses were selected by cell sorting for EGFP expression and subjected to Western blot analysis using anti-Bmi1 (F6) and anti–α-tubulin (Ab-1; Oncogene Science) antibodies.

Reverse transcription–PCR. Total RNA extraction and cDNA synthesis were conducted, as described previously (12). Real-time PCR was performed using TaqMan technology and the ABI PRISM 7000 Sequence Detection System (Applied Biosystems). TaqMan probe and primers for *BMI1* (assay ID Hs00180411_m1) and *β-actin* (assay ID Hs99999903_m1) were obtained from TaqMan gene expression assays (Applied Biosystems). To examine the mRNA expression of *INK4A/ARF* genes in SP cells following *BMI1* knockdown, multiplex reverse transcription–PCR (RT-PCR) was performed as described previously (23). PCR for *BMI1* and *β-actin* was conducted using the following primers: *BMI1* (forward 5′-AGC AGC AAT GAC TGT GAT GC-3′, reverse 5′-CAG TCT CAG GTA TCA ACC AG-3′), *β-actin* (forward 5′-ATC CTG CGT CTG GAC CTG GCT GG-3′, reverse 5′-ACA TGC CGG AGC CGT TGT CGA CGA-3′).

Xenograft transplantation. Various numbers of SP and non-SP cells stably expressing shRNA against *BMI1* or *luciferase* were suspended in DMEM and Matrigel (Becton Dickinson; 1:1) and transplanted to NOD/SCID mice (male, 6–10 wk) under anesthesia. *BMI1* knockdown cells and control cells were implanted into the s.c. space on the right and left sides of the back of recipient mice, respectively. To examine whether enforced expression of *BMI1* in SP cells promotes tumorigenesis, 1×10^4 Huh7 SP cells transduced with *BMI1* and *EGFP* retroviruses were also transplanted.

Tumor formation was observed weekly for 14 wk. The transplantation assays were performed in accordance with institutional guidelines for the use of laboratory animals.

Immunohistochemical analysis. The subcutaneous tumors formed in NOD/SCID mice were fixed in formalin and embedded in paraffin. The sections were subjected to H&E staining. For dual immunohistochemical analyses, the sections were stained with anti-EGFP (BD Biosciences Clontech) and anti-BMI1 (F6), followed by incubation with Alexa-488–conjugated goat anti-rabbit IgG and Alexa-555–conjugated goat anti-mouse IgG (Molecular Probes), respectively.

Statistical analysis. Data are presented as the means ± SE. Statistical differences between two groups were analyzed using the Mann-Whitney units test. P values <0.05 were considered significant.

Results

Preferential expression of BMI1 in SP cells. To gain insight into the crucial role of the polycomb gene product BMI1, we first examined the basal expression of BMI1 in the SP population in Huh7 and PLC/PRF/5 cells. Real-time RT-PCR analyses showed that the mRNA expression of *BMI1* was 4.10 ± 0.36-fold and 1.92 ± 0.25-fold higher in Huh7 and PLC/PRF/5 SP cells than in the corresponding non-SP cells, respectively (Fig. 1*A* and *C*). Immunocytochemical analyses confirmed that BMI1 is highly expressed in the nuclei of SP cells rather than the corresponding non-SP cells in both cell lines (Fig. 1*B* and *D*).

Stable knockdown of *BMI1* by shRNA. We next performed loss-of-function analyses of BMI1 *in vitro*. Stable knockdown of *BMI1* in Huh7 and PLC/PRF/5 cells was achieved by lentivirus-mediated delivery of shRNA against *BMI1*. A lentiviral vector expressing shRNA against *luciferase* was used as a control. We obtained stable cell lines expressing shRNA against *BMI1* or *luciferase* by cell sorting using EGFP as a marker for infection. Western blot analysis showed that both sh-*BMI1*-1 and sh-*BMI1*-2 markedly repressed BMI1 expression in both cell lines, although sh-*BMI1*-1 was less effective than sh-*BMI1*-2 (Fig. 2*A*). Both shRNA inhibited the growth of HCC cell lines. In good agreement with the Western blot data, sh-*BMI1*-2 was more effective in growth suppression than sh-*BMI1*-1 (Fig. 2*B* and *C*). The viability of cells expressing shRNA against *BMI1* was comparable with that of control cells (data not shown).

Detection and isolation of SP cells. SP cell analysis and sorting were performed in Huh7 and PLC/PRF/5 cells stably expressing shRNA against *BMI1* (Fig. 3 and Supplementary Fig. S1). *BMI1* knockdown using sh-*BMI1*-2 considerably decreased the size of the SP population from 0.67 ± 0.09% to 0.19 ± 0.03% in Huh7 cells and from 0.87 ± 0.10% to 0.40 ± 0.04% in PLC/PRF/5 cells (Fig. 3). On the other hand, *BMI1* knockdown using sh-*BMI1*-1 slightly decreased the percentage of SP cells from 0.59 ± 0.04% to 0.32 ± 0.03% in Huh7 cells and from 0.82 ± 0.06% to 0.47 ± 0.03% in PLC/PRF/5 cells (Supplementary Fig. S1). The SP population showed a drastic reduction in number on treatment with the calcium channel blocker verapamil.

Stable overexpression of *BMI1* by retroviral vector. Next, we tested the overexpression of *BMI1* in HCC cells (Supplementary Fig. S2*A*). In clear contrast with the knockdown experiment, the SP subpopulation increased nearly 8-fold with the overexpression of *BMI1* in Huh7 cells (Supplementary Fig. S2*B*). Next, we examined the tumorigenicity of Huh7 SP cells transduced with *BMI1* in NOD/SCID xenograft transplantation. The implantation of 1×10^4 SP cells transduced with *BMI1* resulted in early onset and aggressive

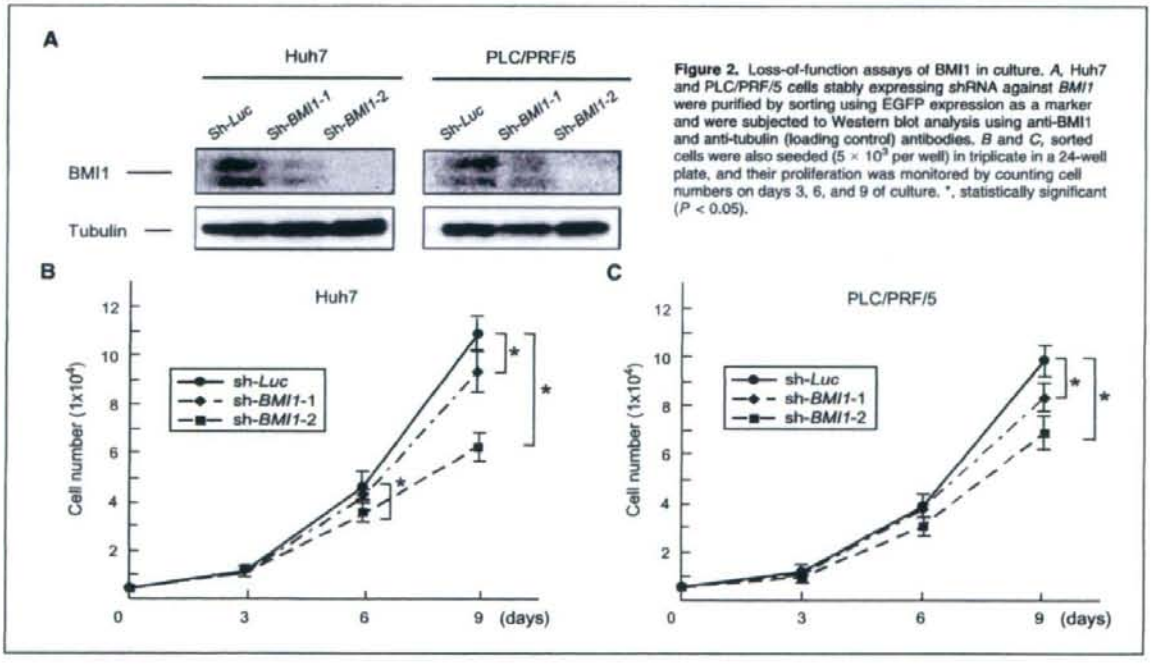

Figure 2. Loss-of-function assays of BMI1 in culture. *A*, Huh7 and PLC/PRF/5 cells stably expressing shRNA against *BMI1* were purified by sorting using EGFP expression as a marker and were subjected to Western blot analysis using anti-BMI1 and anti-tubulin (loading control) antibodies. *B* and *C*, sorted cells were also seeded (5×10^3 per well) in triplicate in a 24-well plate, and their proliferation was monitored by counting cell numbers on days 3, 6, and 9 of culture. *, statistically significant ($P < 0.05$).

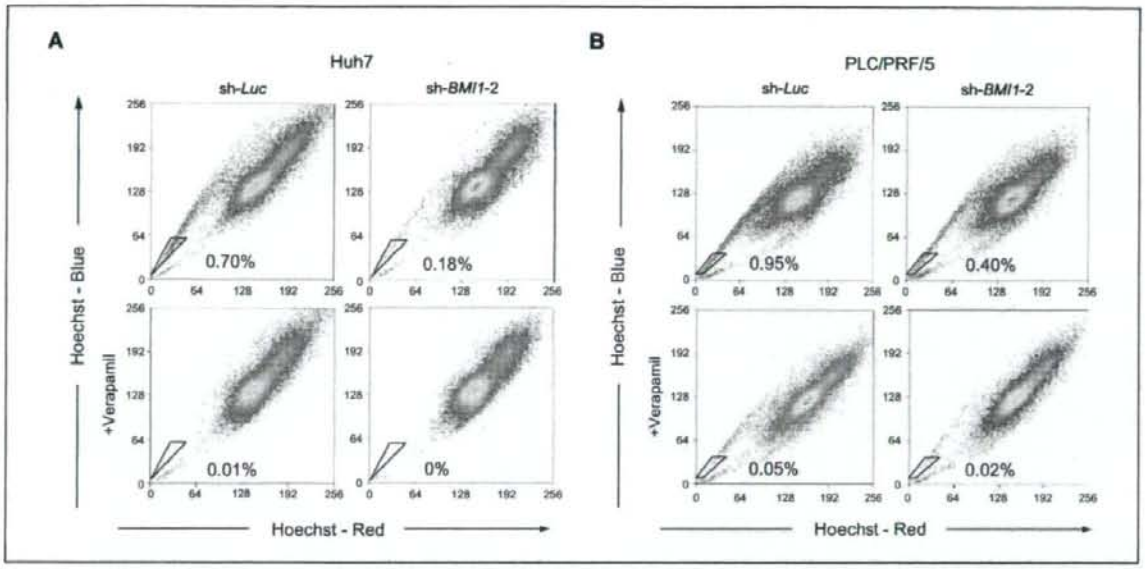

Figure 3. SP cell analysis in *BMI1* knockdown HCC cells by sh-*BMI1*-2. Flow cytometric profiles of SP cells among Huh7 (*A*) and PLC/PRF/5 cells (*B*) after stable knockdown of *BMI1* by sh-*BMI1*-2. SP cell profiles in the presence of verapamil are depicted at the bottom. The percentages of SP cells are indicated.

tumor growth compared with that of control SP cells expressing EGFP (Supplementary Fig. S2*C* and *D*). These results indicated that forced expression of *BMI1* leads to not only enhanced self-renewal but also increased tumorigenicity of SP cells.

Expression of the *INK4A/ARF* gene in *BMI1* knockdown SP cells. To address whether the knockdown of *BMI1* causes derepression of the *INK4A* and *ARF* genes as observed in *Bmi1*-deficient hematopoietic stem cells (HSC; ref. 17), we examined their mRNA expression in SP cells freshly isolated from *BMI1* knockdown and control cells (Fig. 4*A*). In Huh7 SP cells, in which *INK4A* expression is repressed by aberrant DNA methylation in its promoter region (23) and *ARF* is constitutively expressed, *BMI1* knockdown did not affect their expression at all. Conversely, *BMI1* knockdown in PLC/PRF/5 SP cells, in which both *INK4A* and *ARF* are moderately expressed, greatly augmented their expression.

Reanalysis of isolated SP cells. We have previously reported that purified SP cells self-renew and generate nontumorigenic non-SP cells through asymmetrical cell division *in vivo* (12). Purified SP cells repopulate the same hierarchical structure as the original tumor cells consisting of a minor component of SP cells and a major component of non-SP cells (12, 24). This process occurs both *in vitro* and *in vivo*. The SP cells in repopulated tumor retain the same tumor-initiating capacity as the original SP cells. We purified SP cells from both *BMI1* knockdown and control cells and cultured them for 4 weeks to examine the role of BMI1 in this process in culture. The SP subpopulation in *BMI1* knockdown Huh7 cells profoundly decreased (5.5%) compared with that in the control cells (18.8%; Fig. 4*B*). Likewise, the percentage of PLC/PRF/5 SP cells among *BMI1* knockdown and control cells was 6.1% and 22.0%, respectively (Fig. 4*B*). These results imply that BMI1 regulates the self-renewal capability of tumor-initiating SP cells and loss of BMI1 accelerates differentiation toward nontumorigenic non-SP cells.

The role for BMI1 in the maintenance of tumorigenic CD133-positive Huh7 cells. It has been reported that CD133-positive cells possessed greater tumorigenicity than CD133-negative cells in HCC cells, including Huh7 cells (25). Although the majority of Huh7 cells are CD133-positive (Fig. 4*C*), it has been shown that CD133 expression is stronger in SP cells than in non-SP cells (24). We then evaluated the expression of CD133 in the context of BMI1 expression using flow cytometry. *BMI1* knockdown decreased the CD133-positive fraction from 74.2% to 60.9%, whereas *BMI1* overexpression increased it from 71.6% to 84.4% (Fig. 4*C*). These findings indicate that the expression level of BMI1 is tightly correlated with the cancer stem cell phenotype represented not only by SP cells but also by CD133-positive cells.

Tumorigenic ability in xenograft transplantation. To determine whether loss of BMI1 affects the tumorigenicity *in vivo*, various numbers of SP and non-SP cells sorted from the *BMI1* knockdown or control HCC cells were transplanted into NOD/SCID mice (Fig. 5; Table 1). As few as 1×10^3 control SP cells were enough to initiate tumors for both cell lines. In contrast, 1×10^3 *BMI1* knockdown SP cells transduced with sh-*BMI1*-1 and 1×10^4 *BMI1* knockdown SP cells transduced with sh-*BMI1*-2 from Huh7 and PLC/PRF/5 cells failed to initiate subcutaneous tumors in any recipient mice. Tumors derived from control SP cells showed similar histologic features to those formed by the injection of unsorted cells and exhibited the nuclear expression of BMI1 (Fig. 5). Unexpectedly, 1×10^5 *BMI1* knockdown Huh7 and PLC/PRF/5 SP cells with sh-*BMI1*-2 gave rise to tumors in one of three and one of two mice, respectively. However, the tumor size was less than half that of control SP cells. Furthermore,

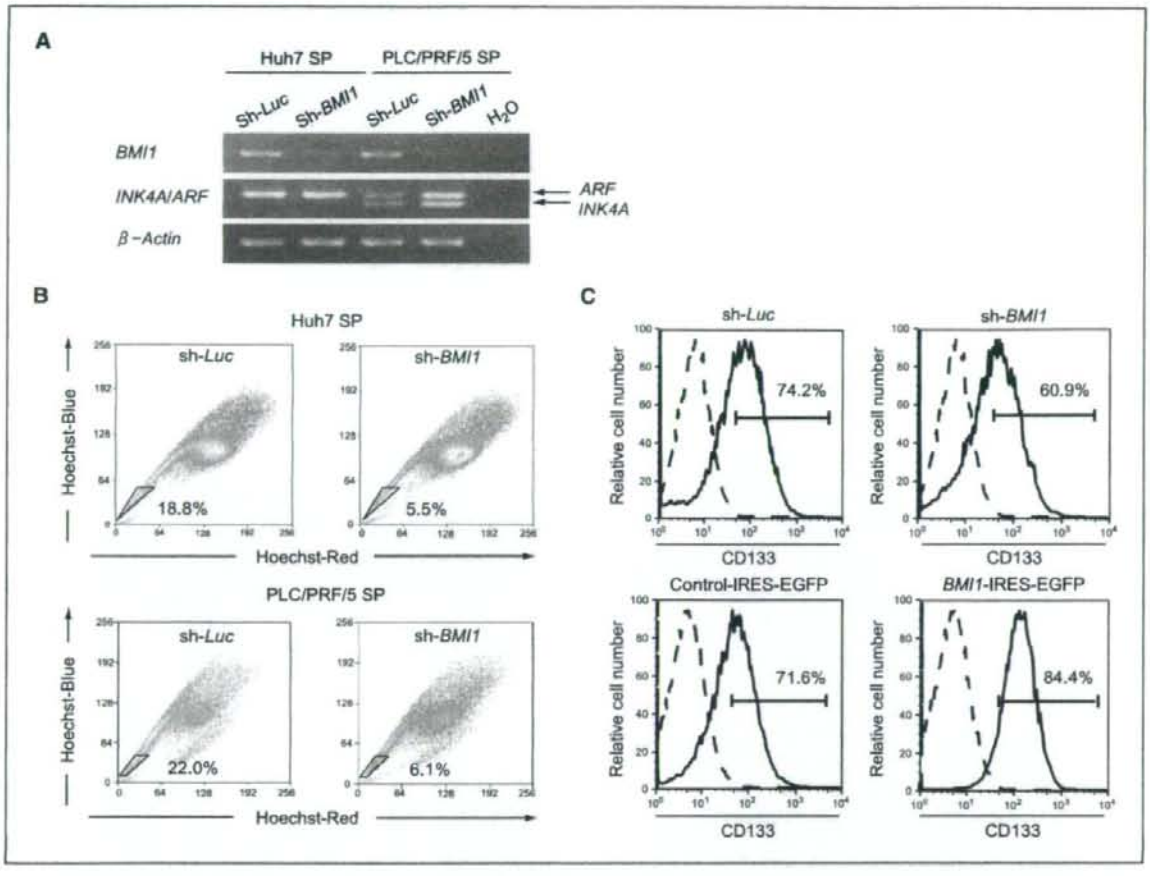

Figure 4. Role of BMI1 in *INK4A/ARF* expression and cancer stem cell phenotype. *A*, RT-PCR analysis of *INK4A/ARF* in *BMI1* knockdown SP cells from Huh7 and PLC/PRF/5 cells. Lane H_2O represents the negative control without the template. *B*, flow cytometric profiles of purified SP cells after culture. SP cells were purified from *BMI1* knockdown cells, cultured for 4 wk, and then subjected to the flow cytometric analysis. *C*, expression of CD133 in *BMI1* knockdown (*top*) and *BMI1* overexpressing cells (*bottom*) detected by flow cytometric analysis. Dotted line represents negative controls. The percentages of CD133-positive cells are indicated.

immunohistochemical analyses revealed that tumors predominantly consisted of contaminating EGFP-negative cells or EGFP-positive cells showing no obvious effects of *BMI1* knockdown (Supplementary Fig. S3). By contrast, tumors derived from control SP cells did not contain EGFP-negative cells at all (Fig. 5). These results further support that the tumor-initiating capacity is profoundly impaired by *BMI1* knockdown. In contrast, the injection of 1×10^6 non-SP cells from either cell line failed to generate tumors in any mice.

Discussion

PcG proteins form chromatin-associated multiprotein complexes, polycomb repressive complex 1 (PRC1) and PRC2 and function as a cellular memory system through epigenetic chromatin modifications (26, 27). Bmi1, a component of PRC1, has been implicated in the regulation of self-renewal in a range of different stem cell systems (28, 29). Of note, Bmi1 is also required for the maintenance of self-renewing leukemic stem cells in a mouse model using *Bmi1*$^{-/-}$ HSCs (30). Recent reports described that BMI1 is preferentially expressed in the tumorigenic subpopulation in breast cancer and head and neck tumors (31, 32). Consistent with these reports, we previously showed that forced expression of *BMI1* promotes the self-renewal of hepatic stem/progenitor cells and contributes to malignant transformation (16). In addition, immunohistochemical analyses showed BMI1 to be overexpressed in >60% of human HCC cases examined.[6] Together, all these findings highlight the importance of BMI1 in hepatocarcinogenesis and implicate BMI1 in the self-renewal of cancer stem cells in HCC.

In the present study, we first examined the basal expression of BMI1 in Huh7 and PLC/PRF/5 SP cells. As expected, both the real-

[6] Unpublished data.

time RT-PCR and immunocytochemical analyses showed BMI1 expression to be stronger in SP cells than non-SP cells in each cell line. We thus directly evaluated the role of BMI1 in cancer stem cell–like SP cells. Lentiviral shRNA-mediated knockdown of *BMI1* allowed a highly efficient loss-of-function assay of the SP subpopulation in culture and in an *in vivo* transplant model. The analysis showed a significant decrease in the frequency of SP cells among the *BMI1* knockdown cells compared with the corresponding control cells. Furthermore, analysis of the growth and differentiation of purified SP cells revealed that loss of BMI1 causes a considerable decrease in the SP subpopulation and facilitates differentiation toward non-SP cells. These results indicated that BMI1 contributes to the self-renewal of SP cells in culture.

Notably, when as few as 1×10^3 control SP cells were sufficient to initiate tumors in NOD/SCID mice, even 10 times more *BMI1* knockdown SP cells (1×10^4) failed to develop tumors. 1×10^5 *BMI1* knockdown SP cells gave increase to tumors in some of the recipient mice, but the tumor-initiating capacity was profoundly reduced. Collectively, the tumorigenic activity in the SP subpopulation seemed to be attenuated nearly 100-fold by the *BMI1* knockdown. Although the important role of Bmi1 in the maintenance of cancer stem cells has already been shown in a mouse leukemia model, this is the first direct evidence that the loss of BMI1 in established cancer stem cells can affect their ability to self-renew and tumorigenicity. The role of BMI1 in the regulation of tumor-initiating SP cells was further supported by the findings of the gain-of-function assay. Although stable knockdown of *BMI1* decreased SP cell numbers *in vitro*, it did not completely abolish SP cells and its effect varied among HCC cell lines. These results strongly indicate that the SP subpopulation is quite heterogeneous, and the contribution of BMI1 to the SP phenotype differs among the cell lines. Considering that BMI1 is just one of multiple self-renewal regulators, the different contributions of molecular machinery, including the Notch, Wnt, and Shh signaling pathways, might also influence the SP phenotype (33). Further analyses would be necessary to clarify the mechanisms underlying the regulation of cancer stem cells in HCC.

Bmi1 regulates the cell cycle, apoptosis and senescence by repressing the *Ink4a/Arf* locus (26, 34). In *Bmi1*-deficient mice, the expression of *Ink4a* and *Arf* is markedly increased in HSCs (17). Conversely, deletion of both *Ink4a* and *Arf* substantially restores the impaired capacity of *Bmi1*$^{-/-}$ HSCs to self-renew (22). These findings suggest that Bmi1 regulates HSCs by acting as a critical failsafe against the premature loss of HSCs induced by Ink4a and Arf-dependent senescence pathways. On the other hand, the Ink4a-Rb and Arf-p53–dependent cellular senescence pathways play a critical role in the triggering of oncogene-induced senescence, which is of substantial importance to the elimination of transforming cells that potentially develop into cancer stem cells (26, 35). In the present study, the expression of the *INK4A* and *ARF* genes was augmented by *BMI1* knockdown in PLC/PRF/5 cells. In this case, derepression of *INK4A* and *ARF* could account for the impaired self-renewal of PLC/PRF/5 SP cells with *BMI1* knockdown. On the other hand, knockdown of *BMI1* in Huh7 cells resulted in no remarkable changes in *INK4A* and *ARF* gene expression compared with the control. Given that the function of p53 is impeded by mutations in Huh7 cells (36), additional targets for BMI1 other than the *INK4A/ARF* locus might be responsible for

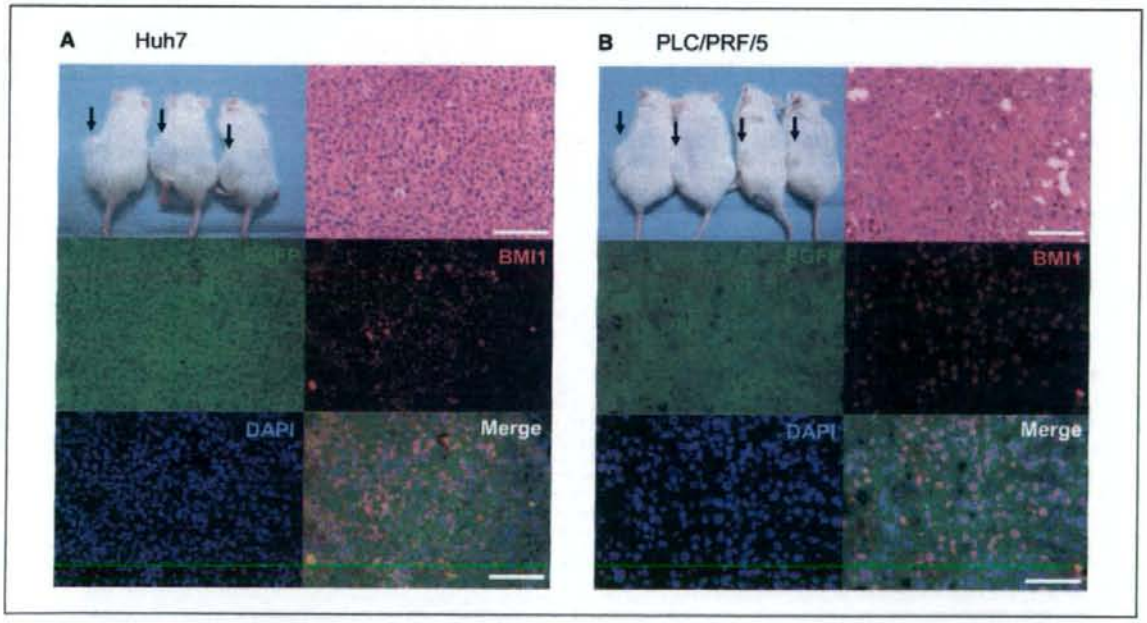

Figure 5. Loss of tumorigenicity in SP cells by *BMI1* knockdown. 1×10^3 control SP cells from Huh7 (*A*) and PLC/PRF/5 cells (*B*) generated tumors in the left subcutaneous space of recipient mice (*arrows*), whereas *BMI1* knockdown SP cells failed to initiate tumors in the right space. Immunohistochemical analyses revealed the nuclear localization of BMI1 in tumor cells generated by control SP cells. *Scale bar*, 100 μm.